New physics effects on $\Lambda_b \to \Lambda_c^* \tau \bar{\nu}_\tau$ decays

Meng-Lin Du,[1] Neus Penalva,[1] Eliecer Hernández,[2] and Juan Nieves[1]
[1]*Instituto de Física Corpuscular (centro mixto CSIC-UV), Institutos de Investigación de Paterna, C/Catedrático José Beltrán 2, E-46980 Paterna, Valencia, Spain*
[2]*Departamento de Física Fundamental e IUFFyM, Universidad de Salamanca, Plaza de la Merced s/n, E-37008 Salamanca, Spain*

(Received 22 July 2022; accepted 23 August 2022; published 26 September 2022)

We benefit from a recent lattice determination of the full set of vector, axial and tensor form factors for the $\Lambda_b \to \Lambda_c^*(2595)\tau\bar{\nu}_\tau$ and $\Lambda_c^*(2625)\tau\bar{\nu}_\tau$ semileptonic decays to study the possible role of these two reactions in lepton flavor universality violation studies. Using an effective theory approach, we analyze different observables that can be accessed through the visible kinematics of the charged particles produced in the tau decay, for which we consider the $\pi^-\nu_\tau, \rho^-\nu_\tau$ and $\mu^-\bar{\nu}_\mu\nu_\tau$ channels. We compare the results obtained in the Standard Model and other schemes containing new physics (NP) interactions, with either left-handed or right-handed neutrino operators. We find a discriminating power between models similar to the one of the $\Lambda_b \to \Lambda_c$ decay, although somewhat hindered in this case by the larger errors of the $\Lambda_b \to \Lambda_c^*$ lattice form factors. Notwithstanding this, the analysis of these reactions is already able to discriminate between some of the NP scenarios and its potentiality will certainly improve when more precise form factors are available.

DOI: 10.1103/PhysRevD.106.055039

I. INTRODUCTION

The experimental observation of the Higgs boson by the ATLAS [1] and CMS [2] collaborations announced the completion of the electroweak sector of the Standard Model (SM). Despite its enormous success in describing many different experimental data, there are however theoretical indications (see for instance chapter 10 of Ref. [3]) as well as experimental measurements that hint at the possibility of the SM being just a low energy effective limit of a more fundamental underlying theory. One of the predictions of the SM is lepton flavor universality (LFU), which implies that the couplings to the W and Z gauge bosons is the same for all three lepton families. However, this prediction is being challenged by different semileptonic decays mediated by charged currents (CC) involving the third lepton and quark generation, i.e. by $b \to c\tau^-\bar{\nu}_\tau$ transitions. The strongest evidence in the direction of LFU violation comes from the ratios $\mathcal{R}_{D^{(*)}} = \frac{\Gamma(\bar{B}\to D^{(*)}\tau^-\bar{\nu}_\tau)}{\Gamma(\bar{B}\to D^{(*)}\mu^-\bar{\nu}_\mu)}$ measured by the *BABAR* [4,5], Belle [6–9] and LHCb [10–12] collaborations. Their combined analysis by the HFLAV collaboration indicates a 3.1σ tension with SM predictions [13]. LHCb [14] has also measured the ratio $\mathcal{R}_{J/\psi} = \Gamma(\bar{B}_c \to J/\psi\tau\bar{\nu}_\tau)/\Gamma(\bar{B}_c \to J/\psi\mu\bar{\nu}_\mu)$, which deviates from the SM predictions [15–27] at the 1.8σ level. If these differences were finally confirmed they would be a clear indication for the necessity of new physics (NP) beyond the SM.

A model-independent way to approach this problem is to take a phenomenological point of view and to carry out an effective field theory analysis, which includes the most general $b \to c\tau^-\bar{\nu}_\tau$ dimension-six operators (for one of the pioneering works on this type of approaches, see Ref. [28]). These operators are assumed to be generated by physics beyond the SM. Their strengths are encoded into unknown Wilson coefficients (WCs) that can be determined by fitting to experimental data. In order to constrain and/or determine the most plausible extension of the SM, observables beyond the above-mentioned LFU ratios need to be considered. Those observables typically include the averaged tau-polarization asymmetry and the longitudinal D^* polarization, which have also been measured by Belle [8,29], the τ forward-backward asymmetry and the upper bound of the $\bar{B}_c \to \tau\bar{\nu}_\tau$ leptonic decay rate [30]. A large number of studies along these lines have been conducted, not only for the $\bar{B} \to D^{(*)}$ [28,31–50] and $\bar{B}_c \to J/\psi, \eta_c$ [23,25,50–52] semileptonic decays, but also for the $\Lambda_b \to \Lambda_c$ transition [39,42,49,53–65], where a similar behavior is to be expected. A better discriminating power for different models could be achieved if four body reactions, involving for instance $D^* \to D\pi, D\gamma$ [33–36,41,45,48] or $\Lambda_c \to \Lambda\pi$ [61,63] decays of the final hadron, are analyzed.

Very recently, the LHCb collaboration has reported a measurement of the $\mathcal{R}_{\Lambda_c} = \frac{\Gamma(\Lambda_b \to \Lambda_c \tau^- \bar{\nu}_\tau)}{\Gamma(\Lambda_b \to \Lambda_c \mu^- \bar{\nu}_\mu)}$ ratio [66] and the experimental value $\mathcal{R}_{\Lambda_c} = 0.242 \pm 0.026 \pm 0.040 \pm 0.059$ turns out to be in agreement, within errors, with the SM prediction $\mathcal{R}^{\rm SM}_{\Lambda_c} = 0.332 \pm 0.007 \pm 0.007$ [67]. The τ^- lepton was reconstructed using the hadronic $\tau^- \to \pi^-\pi^+\pi^-(\pi^0)\nu_\tau$ decay, with the same technique used by the LHCb experiment to obtain $\mathcal{R}_{D^*} = 0.291 \pm 0.019 \pm 0.026 \pm 0.013$ [12], also in agreement with the SM prediction. A higher value $\mathcal{R}_{D^*} = 0.336 \pm 0.027 \pm 0.030$, however, was obtained by the same experiment when the τ lepton was reconstructed using its leptonic decay into a muon [10]. It is then of great interest to see if the above result for the $\Lambda_b \to \Lambda_c$ decay is confirmed or not when the muonic reconstruction channel is used. Such an analysis is under way [68]. As already discussed in Ref. [69], the different deviation of the present $\mathcal{R}_{\Lambda_c}$ and $R_{D^{(*)}}$ ratios with respect to their SM values, suppression for $\mathcal{R}_{\Lambda_c}$ versus enhancement for $R_{D^{(*)}}$, puts a very stringent test on NP extensions of the SM, since scenarios leading to different deviations from SM expectations seem to be required. In this respect, in the very recent work of Ref. [70], it is argued that a more consistent comparison with the SM prediction for $\mathcal{R}_{\Lambda_c}$ is achieved if the recent $\Gamma(\Lambda_b \to \Lambda_c \tau^- \bar{\nu}_\tau)$ LHCb measurement is normalized against the SM value for $\Gamma(\Lambda_b \to \Lambda_c \mu^- \bar{\nu}_\mu)$ instead of the old LEP data used by the LHCb collaboration. This analysis gives rise to a new $\mathcal{R}_{\Lambda_c} = |0.04/V_{cb}|^2(0.285 \pm 0.073)$ value [70], also in agreement with the SM but with a less suppressed central value.

In Refs. [69,71] the $\Lambda_b \to \Lambda_c \tau^- \bar{\nu}_\tau$ and the $\bar{B} \to D^{(*)} \tau^- \bar{\nu}_\tau$ decays were analyzed by employing the $\tau^- \to \pi^- \nu_\tau, \rho^- \nu_\tau$ and $\tau^- \to \mu^- \bar{\nu}_\mu \nu_\tau$ reconstruction channels. There, special attention is paid to different quantities that can be measured by looking just at the visible kinematics of the charged particle produced in the τ decay [71]. Given a good-statistics measurement of these visible distributions, one has access to the values of the unpolarized differential decay width $d\Gamma_{\rm SL}(\omega)/d\omega$ and the spin $\langle P_L^{\rm CM}\rangle(\omega), \langle P_T^{\rm CM}\rangle(\omega)$, angular $A_{FB}(\omega), A_Q(\omega)$, and angular-spin $Z_L(\omega), Z_\perp(\omega), Z_Q(\omega)$ asymmetries. Here ω is the product of the two hadron four-velocities. As shown in Ref. [71], in the absence of CP violation, the above quantities provide the maximal information that can be extracted from the analysis of the semileptonic $H_b \to H_c \tau^- \bar{\nu}_\tau$ decay for a polarized final τ. The general expression that links the visible-kinematics differential distributions to the above given asymmetries was first given in Ref. [72] for the $\tau \to \pi^- \nu_\tau, \rho^- \nu_\tau$ hadronic decay modes. Actually, these hadronic channels are more convenient to determine all the above asymmetries and the role of the latter in distinguishing among different extensions of the SM was analyzed in detail in Refs. [49,71]. Since the full visible-kinematics differential decay width may suffer from low statistics, possible statistically enhanced distributions, which can be obtained by integrating in one or more of the related visible-kinematics variables, are analyzed in Ref. [69] in the search for NP.

In the present work, we will extend these kinds of studies to the $\Lambda_b \to \Lambda_c^*(2595)$ and $\Lambda_b \to \Lambda_c^*(2625)$ semileptonic decays, with the help of the recent lattice chromodynamics (LQCD) determination of the full set of vector, axial and tensor form factors for these two transitions [73,74]. These two isoscalar odd parity resonances, with $J^P = \frac{1}{2}^-$ and $\frac{3}{2}^-$ respectively, are promising candidates for the lightest charmed baryon heavy-quark-spin doublet [75,76].[1] The LFU analysis of the transitions involving these excited baryons could provide valuable/complementary information on the possible existence of NP beyond the SM and on its preferred extensions. The LQCD form factors in Refs. [73,74] are defined based on a helicity decomposition of the amplitudes. After extrapolation to the physical point (both the continuum and the physical pion mass limits), each form factor was parametrized in terms of ω as $f(\omega) = F^f + A^f(\omega - 1)$, corresponding to the first order Taylor expansion around the zero recoil point ($\omega = 1$). That was appropriate since lattice data were only available for just two kinematics near zero recoil. Thus, one expects this parametrization to be reliable only for small values of $(\omega - 1)$ and, in accordance, we shall restrict our evaluation of the different observables to a certain kinematical region near zero recoil.

This work is organized as follows: in Sec. II we will introduce the most general effective Hamiltonian of all possible dimension-six operators for the semileptonic $b \to c$ transitions. We give general analytical results valid for the production of any lepton in the final state, although it is generally assumed that the WCs are nonzero only for the third quark and lepton generation. We also provide the general expression for the transition amplitude squared for the production of a charged lepton in a given polarization state. In Sec. III we present the general formula for the visible-kinematics differential decay width for the sequential $H_b \to H_c \tau^- (\pi^- \nu_\tau, \rho^- \nu_\tau, \mu^- \bar{\nu}_\mu \nu_\tau) \bar{\nu}_\tau$ decays and the expressions after integration in one or more of the related variables. The results and the discussion are presented in Sec. IV. In Appendices A and B we collect the matrix elements (form factor decomposition) and the $\tilde{W}_\chi$ structure functions needed to construct the hadron tensors for the $1/2^+ \to 1/2^-$ and $1/2^+ \to 3/2^-$ transitions, respectively.

II. $H_b \to H_c \ell^- \bar{\nu}_\ell$ EFFECTIVE HAMILTONIAN AND DECAY AMPLITUDE

Following Ref. [45], we use an effective low energy Hamiltonian that includes all dimension-six semileptonic $b \to c$ operators with both left-handed (L) and right-handed (R) neutrino fields,

[1] Some doubts on this respect have recently been put forward [77,78], and experimental distributions for the semileptonic decay of the ground-state bottom baryon Λ_b into both excited states would definitely contribute to shed light into this issue [76].

$$H_{\rm eff} = \frac{4G_F V_{cb}}{\sqrt{2}}[(1+C_{LL}^V)\mathcal{O}_{LL}^V + C_{RL}^V\mathcal{O}_{RL}^V + C_{LL}^S\mathcal{O}_{LL}^S + C_{RL}^S\mathcal{O}_{RL}^S + C_{LL}^T\mathcal{O}_{LL}^T + C_{LR}^V\mathcal{O}_{LR}^V + C_{RR}^V\mathcal{O}_{RR}^V + C_{LR}^S\mathcal{O}_{LR}^S + C_{RR}^S\mathcal{O}_{RR}^S + C_{RR}^T\mathcal{O}_{RR}^T] + \text{H.c.}, \quad (1)$$

with[2]

$$\mathcal{O}_{(L,R)L}^V = (\bar{c}\gamma^\mu b_{L,R})(\bar{\ell}\gamma_\mu \nu_{\ell L}), \qquad \mathcal{O}_{(L,R)L}^S = (\bar{c} b_{L,R})(\bar{\ell}\nu_{\ell L}), \qquad \mathcal{O}_{LL}^T = (\bar{c}\sigma^{\mu\nu} b_L)(\bar{\ell}\sigma_{\mu\nu}\nu_{\ell L}), \quad (3)$$

$$\mathcal{O}_{(L,R)R}^V = (\bar{c}\gamma^\mu b_{L,R})(\bar{\ell}\gamma_\mu \nu_{\ell R}), \qquad \mathcal{O}_{(L,R)R}^S = (\bar{c} b_{L,R})(\bar{\ell}\nu_{\ell R}), \qquad \mathcal{O}_{RR}^T = (\bar{c}\sigma^{\mu\nu} b_R)(\bar{\ell}\sigma_{\mu\nu}\nu_{\ell R}), \quad (4)$$

and where $\psi_{R,L} = (1 \pm \gamma_5)\psi/2$, $G_F = 1.166 \times 10^{-5}\,\text{GeV}^{-2}$, and V_{cb} is the corresponding Cabibbo-Kobayashi-Maskawa matrix element.

The ten, complex in general, WCs C_{AB}^X ($X = S, V, T$, and $A, B = L, R$) parametrize the deviations from the SM. They could be lepton and flavor dependent although they are generally assumed to be nonzero only for the third quark and lepton generation.

The transition amplitude for a $H_b \to H_c \ell^- \bar{\nu}_\ell$ decay can be written, in a short-hand notation, as

$$\mathcal{M} = (J_H^\alpha J_\alpha^L + J_H J^L + J_H^{\alpha\beta} J_{\alpha\beta}^L)_{\nu_{\ell L}} + (J_H^\alpha J_\alpha^L + J_H J^L + J_H^{\alpha\beta} J_{\alpha\beta}^L)_{\nu_{\ell R}}, \quad (5)$$

where the two contributions correspond to the two different neutrino chiralities. In the $m_{\nu_\ell} = 0$ limit there is no interference between these two terms and $|\mathcal{M}|^2$ is given by an incoherent sum of $\nu_{\ell L}$ and $\nu_{\ell R}$ contributions.

The lepton currents for a fully polarized charged lepton are given by

$$J_{\chi,hS}^{L(\alpha\beta)} = \frac{1}{\sqrt{2}}\bar{u}_\ell^S(k';h)\Gamma^{(\alpha\beta)}P_5^{h_\chi}v_{\bar{\nu}_\ell}(k), \qquad \Gamma^{(\alpha\beta)} = 1, \gamma^\alpha, \sigma^{\alpha\beta}, \qquad P_5^{h_\chi} = \frac{1+h_\chi\gamma_5}{2}, \quad (6)$$

with $u_\ell^S(k';h)$ the spinor of the final charged lepton corresponding to a state with $h = \pm 1$ polarization (covariant spin) along a certain four-vector S^α.[3] $h_\chi = \pm 1$ accounts for the two possible neutrino chiralities ($h_\chi = -1$ and $+1$ for $\chi = L$ and $\chi = R$, respectively) considered in the effective Hamiltonian. From the lepton currents one can readily obtain the corresponding lepton tensors needed to evaluate $|\mathcal{M}|^2$. They are constructed as

$$L_{\chi,hS}^{(\alpha\beta)(\rho\lambda)} = J_{\chi,hS}^{L(\alpha\beta)}(J_{\chi,hS}^{L(\rho\lambda)})^* = \frac{1}{2}\text{Tr}[(\not{k}' + m_\ell)\Gamma^{(\alpha\beta)}P_5^{h_\chi}\not{k}\gamma^0\Gamma^{(\rho\lambda)\dagger}\gamma^0 P_S^h], \quad (8)$$

where we have taken $m_{\nu_\ell} = 0$ and P_S^h stands for the projector

$$P_S^h = \frac{1+h\gamma_5\not{S}}{2}. \quad (9)$$

The final expressions for the lepton tensors have been collected in Appendix B of Ref. [71].

The dimensionless hadron currents are given by

$$J_{Hrr'\chi(=L,R)}^{(\alpha\beta)}(p,p') = \langle H_c; p', r'|\bar{c}(0)O_{H\chi}^{(\alpha\beta)}b(0)|H_b; p, r\rangle, \quad (10)$$

with the hadron states normalized as $\langle \vec{p}', r'|\vec{p}, r\rangle = (2\pi)^3(E/M)\delta^3(\vec{p}-\vec{p}')\delta_{rr'}$ and where r, r' represent the spin index. The different $O_{H\chi}^{(\alpha\beta)}$ operator structures are

$$O_{H\chi}^{(\alpha\beta)} = (C_\chi^S + h_\chi C_\chi^P\gamma_5), \qquad (C_\chi^V\gamma^\alpha + h_\chi C_\chi^A\gamma^\alpha\gamma_5), \qquad C_\chi^T\sigma^{\alpha\beta}(1+h_\chi\gamma_5). \quad (11)$$

The WCs above are obtained as linear combinations of those introduced in the effective Hamiltonian in Eq. (1) and

[2]Note that tensor operators with different lepton and quark chiralities vanish identically. It directly follows from

$$\sigma^{\mu\nu}(1+h_\chi\gamma_5)\otimes\sigma_{\mu\nu}(1+h_{\chi'}\gamma_5) = (1+h_\chi h_{\chi'})\sigma^{\mu\nu}\otimes\sigma_{\mu\nu} - (h_\chi + h_{\chi'})\frac{i}{2}\epsilon^{\mu\nu}{}_{\alpha\beta}\sigma^{\alpha\beta}\otimes\sigma_{\mu\nu}, \quad (2)$$

where we use the convention $\epsilon_{0123} = +1$.

[3]This $u_\ell^S(k';h)$ spinor is defined by the condition

$$\gamma_5\not{S}u_\ell^S(k';h) = hu_\ell^S(k';h), \quad (7)$$

where the four-vector S^α satisfies the constraints $S^2 = -1$ and $S\cdot k' = 0$. A helicity state corresponds to $S^\alpha = (|\vec{k}'|, k'^0\hat{k}')/m_\ell$, with $\hat{k}' = \vec{k}'/|\vec{k}'|$ and m_ℓ the charged lepton mass.

their expressions can be found in Appendix A of Ref. [71]. The hadron tensors that enter the evaluation of $|\mathcal{M}|^2$ are defined as

$$W_\chi^{(\alpha\beta)(\rho\lambda)} = \overline{\sum_{r,r'}} \langle H_c; p', r'|\bar{c}(0) O_{H_\chi}^{(\alpha\beta)} b(0)|H_b; p, r\rangle \times \langle H_b; p, r|\bar{b}(0)\gamma^0 O_{H_\chi}^{(\rho\lambda)\dagger}\gamma^0 c(0)|H_c; p', r'\rangle, \tag{12}$$

where we sum (average) over the spin of the final (initial) hadron. As discussed in detail in Ref. [65], the use of Lorentz, parity and time-reversal transformations of the hadron currents and states [79] allows one to write general expressions for the hadron tensors valid for any $H_b \to H_c$ transition. They are linear combinations of independent tensor and pseudotensor structures, constructed out of the vectors p^μ, q^μ, the metric tensor $g^{\mu\nu}$ and the Levi-Civita pseudotensor $\epsilon^{\mu\nu\delta\eta}$. The coefficients of the independent structures are scalar functions of the four-momentum transferred squared q^2, denoted by $\widetilde{W}_\chi$ as introduced in Ref. [71]. The different $\widetilde{W}_\chi$ scalar structure functions (SFs) depend on the WCs $C_\chi^{V,A,S,P,T}$ and on the genuine hadronic responses, the matrix elements of the involved hadron operators which can be derived from the form factors parametrizing each particular transition. It is shown in Refs. [65,71] that there is a total of 16 independent $\widetilde{W}_\chi$ SFs for each neutrino chirality, with the $\widetilde{W}_R$ SFs directly obtained from the $\widetilde{W}_L$ ones by the replacements $C_{\chi=L}^{V,A,S,P,T} \to C_{\chi=R}^{V,A,S,P,T}$. The different $W_\chi^{(\alpha\beta)(\rho\lambda)}$ hadron tensors, together with the definition of the $\widetilde{W}_\chi$ SFs are compiled in Appendix C of Ref. [71].

As shown here in Appendix A, the $\widetilde{W}_\chi$ SFs for the $\Lambda_b \to \Lambda_c^*[J^P = \frac{1}{2}^-]$ transition can be easily obtained from those in Appendix C of Ref. [71] by replacing $C_\chi^V \leftrightarrow C_\chi^A$ and $C_\chi^S \leftrightarrow C_\chi^P$. In addition, the genuine hadron $W_{i=1,2,4,5}^{VV,AA}$, $W_{i=3}^{VA}$, $W_{1,2,3,4,5}^{T}$, W_S, W_P, $W_{I1,I2}^{VS,AP}$, $W_{I3}^{ST,PpT}$ and $W_{I4,I5,I6,I7}^{VT,ApT}$ SFs, which are independent of the WCs, can be read out from Eqs. (E3)–(E5) of Ref. [65] for the $\Lambda_b \to \Lambda_c$ transition.[4]

On the other hand, the $\widetilde{W}_\chi$ SFs for the $\Lambda_b \to \Lambda_c^*[J^P = \frac{3}{2}^-]$ decay are explicitly calculated in this work and they are given in Eqs. (B25)–(B41) of Appendix B.

Going back to the amplitude squared, it was shown in Refs. [49,65] that for the production of a charged lepton with polarization h along the four-vector S^α, and for massless neutrinos, one has that

$$\frac{2\bar{\Sigma}|\mathcal{M}|^2}{M^2} = \frac{2\bar{\Sigma}(|\mathcal{M}|^2_{\nu_{\ell L}} + |\mathcal{M}|^2_{\nu_{\ell R}})}{M^2} = \mathcal{N}(\omega, p\cdot k) + h\left\{\frac{(p\cdot S)}{M}\mathcal{N}_{\mathcal{H}_1}(\omega, p\cdot k) + \frac{(q\cdot S)}{M} \times \mathcal{N}_{\mathcal{H}_2}(\omega, p\cdot k) + \frac{\epsilon^{Sk'qp}}{M^3}\mathcal{N}_{\mathcal{H}_3}(\omega, p\cdot k)\right\}, \tag{13}$$

where we have summed (averaged) over the polarization state of the final (initial) hadron. As already mentioned, ω is the product of the two hadron four-velocities and it is related to q^2 via $q^2 = M^2 + M'^2 - 2MM'\omega$, with M (M') the mass of the initial (final) hadron. Besides, we have made use of the notation $\epsilon^{Sk'qp} = \epsilon^{\alpha\beta\rho\lambda} S_\alpha k'_\beta q_\rho p_\lambda$. As for the $\mathcal{N}$ and $\mathcal{N}_{\mathcal{H}_{123}}$ scalar functions, they are given by

$$\begin{aligned}
\mathcal{N}(\omega, k\cdot p) &= \frac{1}{2}\left[\mathcal{A}(\omega) + \mathcal{B}(\omega)\frac{(k\cdot p)}{M^2} + \mathcal{C}(\omega)\frac{(k\cdot p)^2}{M^4}\right],\\
\mathcal{N}_{\mathcal{H}_1}(\omega, k\cdot p) &= \mathcal{A}_\mathcal{H}(\omega) + \mathcal{C}_\mathcal{H}(\omega)\frac{(k\cdot p)}{M^2},\\
\mathcal{N}_{\mathcal{H}_2}(\omega, k\cdot p) &= \mathcal{B}_\mathcal{H}(\omega) + \mathcal{D}_\mathcal{H}(\omega)\frac{(k\cdot p)}{M^2} + \mathcal{E}_\mathcal{H}(\omega)\frac{(k\cdot p)^2}{M^4},\\
\mathcal{N}_{\mathcal{H}_3}(\omega, k\cdot p) &= \mathcal{F}_\mathcal{H}(\omega) + \mathcal{G}_\mathcal{H}(\omega)\frac{(k\cdot p)}{M^2}.
\end{aligned} \tag{14}$$

The term $\mathcal{N}_{\mathcal{H}_3}$ is proportional to the imaginary part of SFs, which requires the existence of relative phases between some of the complex WCs, thus incorporating violation of the CP symmetry in the NP effective Hamiltonian. The expressions of the $\mathcal{A}, \mathcal{B}, \mathcal{C}, \mathcal{A}_\mathcal{H}, \mathcal{B}_\mathcal{H}, \mathcal{C}_\mathcal{H}, \mathcal{D}_\mathcal{H}, \mathcal{E}_\mathcal{H}, \mathcal{F}_\mathcal{H}$ and $\mathcal{G}_\mathcal{H}$ in terms of the $\widetilde{W}_\chi$ SFs are collected in Appendix D of Ref. [71]. As inferred from Eq. (13), $\mathcal{A}$, $\mathcal{B}$, and $\mathcal{C}$ describe the production of an unpolarized final charged lepton, while $\mathcal{A}_\mathcal{H}, \mathcal{B}_\mathcal{H}, \mathcal{C}_\mathcal{H}, \mathcal{D}_\mathcal{H}, \mathcal{E}_\mathcal{H}, \mathcal{F}_\mathcal{H}$ and $\mathcal{G}_\mathcal{H}$ are also needed for the description of decays with a defined polarization ($h = \pm 1$) of the outgoing charged lepton along the four-vector S^α.

III. SEQUENTIAL $H_b \to H_c\tau^-(\pi^-\nu_\tau, \rho^-\nu_\tau, \mu^-\bar{\nu}_\mu\nu_\tau)\bar{\nu}_\tau$ DECAYS AND VISIBLE KINEMATICS

Due to its short mean life, the τ produced in a $H_b \to H_c\tau^-\bar{\nu}_\tau$ process cannot be directly measured and all the accessible information on the decay is encoded in the visible kinematics of the τ-decay products. The three dominant decay modes $\tau \to \pi\nu_\tau, \rho\nu_\tau$ and $\ell\bar{\nu}_\ell\nu_\tau$ ($\ell = e$, μ) account for more than 70% of the total τ width. The (visible) differential distributions of the charged particle produced in the tau decay have been studied extensively for $\bar{B} \to D^{(*)}$ decays in Refs. [31,72,80–82]. The general expression for the differential decay width for the $H_b \to H_c\tau^-(d\nu_\tau)\bar{\nu}_\tau$ decay, with $d = \pi^-, \rho^-, \ell^-\bar{\nu}_\ell$, reads [71,72,81,82]

[4]Note that the names of the form factors in the parametrizations of Eqs. (A1)–(A6) are chosen in order to directly use the results of Eqs. (E3)–(E5) of Ref. [65].

$$\frac{d^3\Gamma_d}{d\omega d\xi_d d\cos\theta_d} = \mathcal{B}_d \frac{d\Gamma_{\rm SL}}{d\omega}\{F_0^d(\omega,\xi_d) + F_1^d(\omega,\xi_d)\cos\theta_d + F_2^d(\omega,\xi_d)P_2(\cos\theta_d)\}, \quad (15)$$

which is given in terms of ω, $\xi_d = \frac{E_d}{\gamma m_\tau}$ (here $\gamma = \frac{q^2+m_\tau^2}{2m_\tau\sqrt{q^2}}$), which is the ratio of the energies of the tau-decay charged particle and the tau lepton measured in the $\tau^-\bar{\nu}_\tau$ center of mass frame (CM), and θ_d, the angle made by the three-momenta of the final hadron and the tau-decay charged particle measured in the same CM system (see Fig. 1 of Ref. [69]). The azimuthal angular (ϕ_d) distribution of the tau decay charged product is sensitive to possible CP odd effects [$\mathcal{N}_{\mathcal{H}_3}$ term in Eq. (14)]. However, the measurement of ϕ_d would require the full reconstruction of the tau three momentum, and this azimuthal angle has been integrated out to obtain the differential decay width of Eq. (15). That is the reason why the latter visible distribution does not depend on $\mathcal{N}_{\mathcal{H}_3}$, and thus it does not contain any information on possible CP violation contributions to the effective NP Hamiltonian of Eq. (1).

In addition, $\mathcal{B}_d$ in Eq. (15) is the branching ratio for the $\tau^- \to d^-\nu_\tau$ decay mode and $P_2(\cos\theta_d)$ stands for the Legendre polynomial of order 2. As for $d\Gamma_{\rm SL}/d\omega$, it represents the differential decay width for the unpolarized semileptonic $H_b \to H_c\tau^-\bar{\nu}_\tau$ decay. It reads

$$\frac{d\Gamma_{\rm SL}}{d\omega} = \frac{G_F^2|V_{cb}|^2 M'^3 M^2}{24\pi^3}\sqrt{\omega^2-1}\left(1-\frac{m_\tau^2}{q^2}\right)^2 n_0(\omega), \quad (16)$$

where $n_0(\omega)$ contains all the dynamical information, including any possible NP contribution. It is given by $n_0(\omega) = 3a_0(\omega) + a_2(\omega)$, where $a_{0,2}(\omega)$ are linear combinations of $\mathcal{A}(\omega), \mathcal{B}(\omega)$ and $\mathcal{C}(\omega)$, with explicit expressions given in Eq. (18) of Ref. [65]. The $F_{0,1,2}^d(\omega,\xi_d)$ functions in Eq. (15) can be written as [69,72]

$$\begin{aligned}
F_0^d(\omega,\xi_d) &= C_n^d(\omega,\xi_d) + C_{P_L}^d(\omega,\xi_d)\langle P_L^{\rm CM}\rangle(\omega),\\
F_1^d(\omega,\xi_d) &= C_{A_{FB}}^d(\omega,\xi_d)A_{FB}(\omega) + C_{Z_L}^d(\omega,\xi_d)Z_L(\omega)\\
&\quad + C_{P_T}^d(\omega,\xi_d)\langle P_T^{\rm CM}\rangle(\omega),\\
F_2^d(\omega,\xi_d) &= C_{A_Q}^d(\omega,\xi_d)A_Q(\omega) + C_{Z_Q}^d(\omega,\xi_d)Z_Q(\omega)\\
&\quad + C_{Z_\perp}^d(\omega,\xi_d)Z_\perp(\omega),
\end{aligned} \quad (17)$$

where the decay-mode dependent coefficients $C_a^d(\omega,\xi_d)$ are purely kinematical. Their analytical expressions for the $\pi^-\nu_\tau, \rho^-\nu_\tau$ and $\ell^-\bar{\nu}_\ell\nu_\tau$ decay channels can be found in Appendix G of Ref. [71]. The rest of the observables in Eq. (17) are the tau-spin ($\langle P_{L,T}^{\rm CM}\rangle(\omega)$), tau-angular ($A_{FB,Q}(\omega)$) and tau-angular-spin ($Z_{L,Q,\perp}(\omega)$) asymmetries of the $H_b \to H_c\tau\bar{\nu}_\tau$ parent decay. They can be written [65,71] in terms of the $\mathcal{A},\mathcal{B},\mathcal{C},\mathcal{A}_\mathcal{H},\mathcal{B}_\mathcal{H},\mathcal{C}_\mathcal{H},\mathcal{D}_\mathcal{H}$ and $\mathcal{E}_\mathcal{H}$ functions introduced in Eq. (14). A numerical analysis of the role of each of the observables $d\Gamma_{\rm SL}/d\omega$, $\langle P_{L,T}^{\rm CM}\rangle(\omega)$, $A_{FB,Q}(\omega)$ and $Z_{L,Q,\perp}(\omega)$ in the context of LFU violation was conducted for the $\Lambda_b \to \Lambda_c\tau^-\bar{\nu}_\tau$ transition in Refs. [49,71]. Here we perform an analog analysis for the $\Lambda_b \to \Lambda_c^*(2595)$ and $\Lambda_b \to \Lambda_c^*(2625)$ semileptonic decays, for which the only differences are fully encoded in the form-factor input contained in the $\widetilde{W}_\chi$ SFs. This is because the expressions of $\mathcal{A},\mathcal{B},\mathcal{C},\mathcal{A}_\mathcal{H},\mathcal{B}_\mathcal{H},\mathcal{C}_\mathcal{H},\mathcal{D}_\mathcal{H}$ and $\mathcal{E}_\mathcal{H}$ (or equivalently the differential decay width for unpolarized tau, the tau-spin, tau-angular and tau-angular-spin asymmetries) in terms of the latter is independent of the $b \to c$ transition, and they are given by Eqs. (D1) and (D2) of Ref. [71].

Measuring the triple differential decay width in Eq. (15) could also be difficult due to low statistics. An increased statistics is achieved by integrating in one or more of the variables $\cos\theta_d$, ξ_d and ω, at the price that the resulting distributions might not depend on some of the observables in Eq. (17). For instance, accumulating in the polar angle leads to the distribution [83]

$$\frac{d^2\Gamma_d}{d\omega d\xi_d} = 2\mathcal{B}_d\frac{d\Gamma_{\rm SL}}{d\omega}\{C_n^d(\omega,\xi_d) + C_{P_L}^d(\omega,\xi_d)\langle P_L^{\rm CM}\rangle(\omega)\}, \quad (18)$$

from where one can only extract, looking at the dependence on ξ_d, $d\Gamma_{\rm SL}/d\omega$ and the CM τ longitudinal polarization [$\langle P_L^{\rm CM}\rangle(\omega)$]. From the latter, it immediately follows the averaged CM tau longitudinal polarization asymmetry,

$$P_\tau = -\frac{1}{\Gamma_{\rm SL}}\int d\omega \frac{d\Gamma_{\rm SL}}{d\omega}\langle P_L^{\rm CM}\rangle(\omega), \quad (19)$$

which has been measured for the $\bar{B} \to D^*\tau\bar{\nu}_\tau$ decay by the Belle collaboration [8].

Integrating Eq. (15) in the ξ_d variable one obtains the double differential decay width [69]:

$$\frac{d^2\Gamma_d}{d\omega d\cos\theta_d} = \mathcal{B}_d\frac{d\Gamma_{\rm SL}}{d\omega}[\widetilde{F}_0^d(\omega) + \widetilde{F}_1^d(\omega)\cos\theta_d + \widetilde{F}_2^d(\omega)P_2(\cos\theta_d)]. \quad (20)$$

While $\widetilde{F}_0^d(\omega) = 1/2$, losing in this way all information on $\langle P_L^{\rm CM}\rangle(\omega)$, one has that

$$\widetilde{F}_1^d(\omega) = C_{A_{FB}}^d(\omega)A_{FB}(\omega) + C_{Z_L}^d(\omega)Z_L(\omega) + C_{P_T}^d(\omega)\langle P_T^{\rm CM}\rangle(\omega), \quad (21)$$

$$\widetilde{F}_2^d(\omega) = C_{A_Q}^d(\omega)A_Q(\omega) + C_{Z_Q}^d(\omega)Z_Q(\omega) + C_{Z_\perp}^d(\omega)Z_\perp(\omega), \quad (22)$$

which retain all the information on the other six asymmetries, since the kinematical coefficients $C_i^d(\omega)$ are known.

A further integration in ω additionally enhances the statistics. The obtained angular distribution [69],

$$\frac{d\Gamma_d}{d\cos\theta_d} = \mathcal{B}_d\Gamma_{\rm SL}\left[\frac{1}{2} + \widehat{F}_1^d\cos\theta_d + \widehat{F}_2^d P_2(\cos\theta_d)\right],$$
$$\widehat{F}_{1,2}^d = \frac{1}{\Gamma_{\rm SL}}\int_1^{\omega_{\rm max}}\frac{d\Gamma_{\rm SL}}{d\omega}\widetilde{F}_{1,2}^d(\omega)d\omega, \tag{23}$$

could still be a useful observable in the search for NP beyond the SM.

Finally, from the differential decay width $d^2\Gamma_d/(d\omega d\xi_d)$ given in Eq. (18) one can get [69]

$$\frac{d\Gamma_d}{dE_d} = 2\mathcal{B}_d\int_{\omega_{\rm inf}(E_d)}^{\omega_{\rm sup}(E_d)} d\omega\frac{1}{\gamma m_\tau}\frac{d\Gamma_{\rm SL}}{d\omega}\{C_n^d(\omega,\xi_d) + C_{P_L}^d(\omega,\xi_d)\langle P_L^{\rm CM}\rangle(\omega)\}, \tag{24}$$

where the appropriate limits in ω for each of the sequential decays considered are given in Ref. [69].

From the latter distribution one can define the dimensionless observable

$$\widehat{F}_0^d(E_d) = \frac{m_\tau}{2\mathcal{B}_d\Gamma_{\rm SL}}\frac{d\Gamma_d}{dE_d}. \tag{25}$$

Although it is normalized for all channels as

$$\frac{1}{m_\tau}\int_{E_d^{\rm min}}^{E_d^{\rm min}} dE_d\widehat{F}_0^d(E_d) = \frac{1}{2}, \tag{26}$$

its energy dependence is still affected by the CM τ longitudinal polarization $\langle P_L^{\rm CM}\rangle(\omega)$.

Predictions for the $d^2\Gamma/(d\omega d\cos\theta_d)$, $d\Gamma/d\cos\theta_d$ and the $\widehat{F}_0^d(E_d)$ distributions, and their role in distinguishing among different NP models, were presented and discussed in Ref. [69] for the $\Lambda_b\to\Lambda_c\tau^-(\pi^-\nu_\tau,\rho^-\nu_\tau,\mu^-\bar\nu_\mu\nu_\tau)\bar\nu_\tau$ and $\bar B\to D^{(*)}\tau^-(\pi^-\nu_\tau,\rho^-\nu_\tau,\mu^-\bar\nu_\mu\nu_\tau)\bar\nu_\tau$ sequential decays. Here, we will also extend the study to reactions initiated by the $\Lambda_b\to\Lambda_c^*(2595)$ and $\Lambda_b\to\Lambda_c^*(2625)$ semileptonic parent decays.

IV. RESULTS AND DISCUSSION

In this section we present $\Lambda_b\to\Lambda_c^*(2595),\Lambda_c^*(2625)$ results for the observables mentioned in Sec. III above. We will consider SM and different NP scenarios involving left- and right-handed neutrino fields taken from Refs. [42,45]. Since the LQCD form factors from Refs. [73,74] that we use are not reliably obtained at high ω values, we will restrict ourselves to the $1\le\omega\le 1.1$ region. For this latter reason we will not show results for $d\Gamma_d/d\cos\theta_d$ or $\widehat{F}_0^d(E_d)$ since they involve an integration in the ω variable over the full available phase space, including regions for which the LQCD form factors are not reliable.

For each observable, we give central values plus an error band that we construct by adding in quadrature the form-factor and WC uncertainties. For the errors related to the WCs we shall use statistical samples of WCs selected such that the χ^2-merit function computed in Refs. [42,45], for left- and right-handed neutrino NP fits, respectively, changes at most by one unit from its value at the fit minimum (for further details see Sec. III B of Ref. [65]). For the uncertainty associated to the form factors, we consider two different sources [73]: statistical and systematic. We obtain the statistical error using the appropriate covariance matrix to Monte Carlo generate a great number of form factor samples from which we evaluate the corresponding quantity and its standard deviation. The systematic error is evaluated as explained in Sec. VI of Ref. [73]. This latter determination makes use of the form factors obtained with higher-order fits. Statistical and systematic errors are then added in quadrature to get the total error associated to the form factors.

In Figs. 1 and 2 we show, for the $\Lambda_b\to\Lambda_c^*(2595)\tau^-\bar\nu_\tau$ and $\Lambda_b\to\Lambda_c^*(2625)\tau^-\bar\nu_\tau$ decays respectively, the results for $n_0(\omega)$ and the full set of asymmetries introduced in Eq. (17). They have been obtained within the SM and the two NP models corresponding to fits 6 and 7 of Ref. [42]. The latter two models include only left-handed (L) neutrino operators and the corresponding WCs were obtained from fits to the experimental evidences of LFU violations in the B-meson sector. In Table I we give the values corresponding to the C_χ^S, C_χ^P, C_χ^V, C_χ^A and C_χ^T coefficients introduced in Eq. (11) since the $\widetilde{W}_\chi$ hadronic SFs are written in terms of the latter. Even though these two NP scenarios have been adjusted to reproduce the measured $R_{D^{(*)}}$ ratios, they show a different behavior for other quantities. As seen from the figures, L fit 6 and SM results agree within errors for most of the observables, while the predictions from L fit 7 are quite different for the A_{FB}, Z_L, $\langle P_L^{\rm CM}\rangle$ and $\langle P_T^{\rm CM}\rangle$ asymmetries. The latter are thus helpful in distinguishing between these two NP models that otherwise give very similar results for the $R_{D^{(*)}}$ ratios.

In Fig. 3 we compare the results obtained within the SM and fit R S7a of Ref. [45]. The latter includes only NP operators constructed with right-handed (R) neutrino fields, and the corresponding WCs (see Table I) have also been adjusted to reproduce the measured $R_{D^{(*)}}$ ratios. Among the different R fits conducted in Ref. [45], this is one of the more promising in terms of the pull from the SM hypothesis.[5] However, due to the wide error bands, we find no significant difference between the R S7a model and SM results. The exceptions are the Z_L and $\langle P_T^{\rm CM}\rangle$ asymmetries for the $\Lambda_b\to\Lambda_c^*(2595)\tau^-\bar\nu_\tau$ decay. The R S7a and the L fit

[5]This NP scenario considers a scalar leptoquark, with non-vanishing C_{RR}^V, C_{RR}^T and C_{RR}^S and $C_{RR}^S\approx -8C_{RR}^T$. The fit carried out in Ref. [45] leads to a solution dominated by C_{RR}^V, with C_{RR}^T compatible with zero within one sigma.

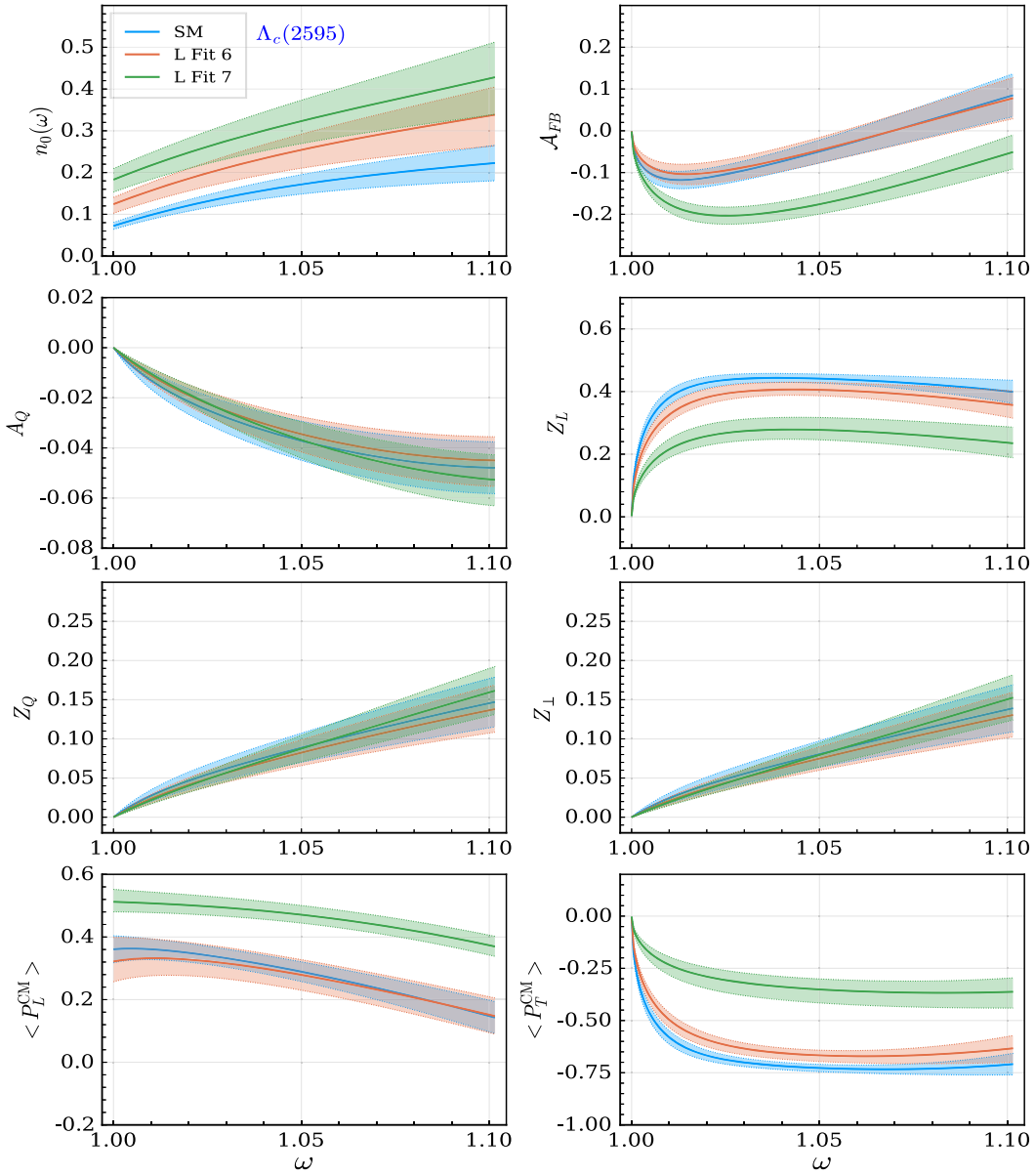

FIG. 1. $d\Gamma_{SL}/d\omega$ differential decay width and $A_{FB}, A_Q, Z_L, Z_Q, Z_\perp, \langle P_L^{CM} \rangle$ and $\langle P_T^{CM} \rangle$ asymmetries evaluated for the $\Lambda_b \to \Lambda_c^*(2595)\tau^-\bar{\nu}_\tau$ decay within the SM and the left-handed neutrino NP models corresponding to fits 6 and 7 of Ref. [42]. The error bands account for uncertainties both in the WCs and form factors, see text for details.

6 models give also similar predictions, agreeing within errors. As for the differences with L fit 7, the best observables to distinguish between the R S7a and the L fit 7 models are the A_{FB} and $\langle P_L^{CM} \rangle$ asymmetries for the $\Lambda_b \to \Lambda_c^*(2595)\tau^-\bar{\nu}_\tau$ decay, whereas for $\Lambda_b \to \Lambda_c^*(2625)\tau^-\bar{\nu}_\tau$ one finds that not only A_{FB} and $\langle P_L^{CM} \rangle$, but also Z_L and $\langle P_T^{CM} \rangle$ are adequate observables.

We show now the results for the $\widetilde{F}_{1,2}^d(\omega)$ coefficient functions that expand the statistically enhanced $d^2\Gamma/(d\omega d\cos\theta_d)$ differential decay width of Eq. (20).[6] In fact, we show the products $n_0(\omega)\widetilde{F}_{1,2}^d(\omega)$ since, as mentioned, $n_0(\omega)$ contains all the dynamical effects included in $d\Gamma_{SL}/d\omega$ which appears as an overall factor of the $d^2\Gamma/(d\omega d\cos\theta_d)$ distribution. Predictions obtained within the SM, and the L fit 7 and the R S7a NP models of Refs. [42,45], respectively, are presented in Fig. 4. As it was to be expected from the previous results, SM and R fit 7a results agree within errors in all cases. Similar results (not shown) are found for L fit 6. However, for most of the observables plotted in the figure, the L fit 7 predictions are distinguishable from those obtained using the SM or R S7a models, either in the near zero-recoil region or in the upper part of the shown ω interval.

[6]Note that $\widetilde{F}_0^d(\omega) = 1/2$ in all cases.

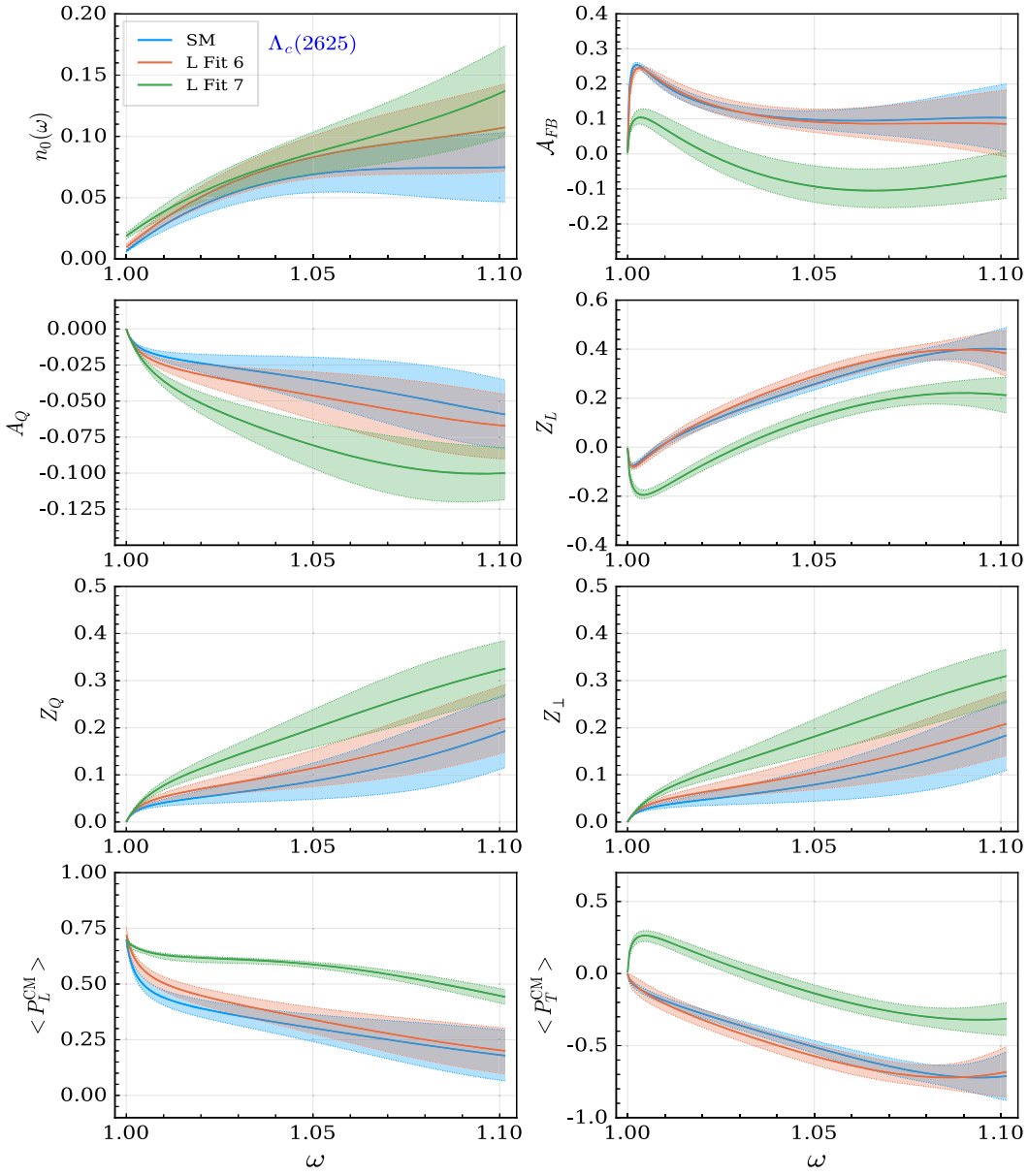

FIG. 2. Same as Fig. 1, but for the $\Lambda_b \to \Lambda_c^*(2625)\tau^-\bar{\nu}_\tau$ decay.

When compared to the $\Lambda_b \to \Lambda_c$ decay considered in Refs. [69,71], we find here a worse discriminating power between different models due to the large errors in the form factors. Nevertheless, with the present values of the latter, these $\Lambda_b \to \Lambda_c^*$ reactions are already able to distinguish between the L fit 7 model of Ref. [42] and the L fit 6 and R S7a models of Refs. [42,45], or between L fit 7 and the SM. A more precise determination of the form factors, with less error and an extended ω region of validity, would certainly increase the value of the $\Lambda_b \to \Lambda_c^*(2595), \Lambda_c^*(2625)$ decays in the search for NP in LFU violation studies.

Focusing on the SM $n_0(\omega)$ distributions in Figs. 1 and 2, we conclude that $\Gamma_{\rm SL}$ (or at least the partially integrated width up to $\omega \leq 1.1$) for the $\Lambda_c^*(2625)$ mode is smaller than for the $\Lambda_c^*(2595)$ final state, contradicting the expectations from heavy-quark spin symmetry [76]. Moreover, comparing with the results displayed in the left-upper plot of Fig. 2 of Ref. [71], both widths are probably around a factor of 10 lower than that of the Λ_b decay into the ground state charmed baryon, $\Lambda_b \to \Lambda_c[J^P = 1/2^+]$. This reduction does not affect the tau-spin, tau-angular and tau-angular-spin asymmetries also shown in these figures, since these observables should not depend on the overall size of the

TABLE I. Wilson coefficients entering in the hadron currents of Eqs. (10) and (11). We collect numerical values for the NP models fitted in Refs. [42] (L fits 6 and 7) and [45] (R S7a). Here $C^{V,A}_{\chi=L} = 1 + C^V_{LL} \pm C^V_{RL}$, $C^{S,P}_{\chi=L} = C^S_{LL} \pm C^S_{RL}$, $C^T_{\chi=L} = C^T_{LL}$, $C^{V,A}_{\chi=R} = C^V_{RR} \pm C^V_{LR}$, $C^{S,P}_{\chi=R} = C^S_{RR} \pm C^S_{LR}$, and $C^T_{\chi=R} = C^T_{RR}$, where the coefficients $C^{S,V,T}_{AB}$ $(A, B = L, R)$ appear directly in the NP effective Hamiltonian of Eq. (1). Note that within the R S7a scalar leptoquark scenario, $C^A_{\chi=R} = C^V_{\chi=R}$ and $C^P_{\chi=R} = C^S_{\chi=R}$ since in that model $C^V_{LR} = C^S_{LR} = 0$ [45].

	$C^S_{\chi=L}$	$C^P_{\chi=L}$	$C^V_{\chi=L}$	$C^A_{\chi=L}$	$C^T_{\chi=L}$	$C^S_{\chi=R}$	$C^V_{\chi=R}$	$C^T_{\chi=R}$
SM	⋯	⋯	1	1	⋯	⋯	⋯	⋯
L fit 6	$-0.16^{+0.10}_{-0.07}$	$-0.26^{+0.00}_{-0.01}$	$1.26^{+0.03}_{-0.04}$	$1.10^{+0.07}_{-0.11}$	$0.01^{+0.02}_{-0.04}$	⋯	⋯	⋯
L fit 7	$-1.32^{+0.15}_{-0.12}$	$-0.22^{+0.01}_{-0.01}$	$1.70^{+0.02}_{-0.02}$	$1.02^{+0.05}_{-0.07}$	$-0.01^{+0.02}_{-0.02}$	⋯	⋯	⋯
R S7a	⋯	⋯	1	1	⋯	$-0.18^{+0.60}_{-0.32}$	$0.42^{+0.03}_{-0.20}$	$0.02^{+0.04}_{-0.08}$

semileptonic width $\Gamma_{\rm SL}$. Actually, the asymmetries provide distinct ω patterns for the Λ_b decay into each of the charmed final state baryons, which have different spin-parity quantum numbers. This makes the comparison of theoretical model predictions, considering jointly all three $[\Lambda_c, \Lambda_c^*(2595), \Lambda_c^*(2625)]$ modes, more exhaustive and demanding.

Next, for some of the observables studied so far, we investigate how the NP operators affect the SM predictions. In Fig. 5, we pay attention to the $n_0(\omega)$ (which equals to $d\Gamma_{\rm SL}/d\omega$ up to a kinematical factor), and the angular-$A_{FB}(\omega)$ and spin- $\langle P^{\rm CM}_{L,T}\rangle(\omega)$ asymmetry distributions. These three observables are commonly discussed in the literature and, presumably, they are amongst the easiest

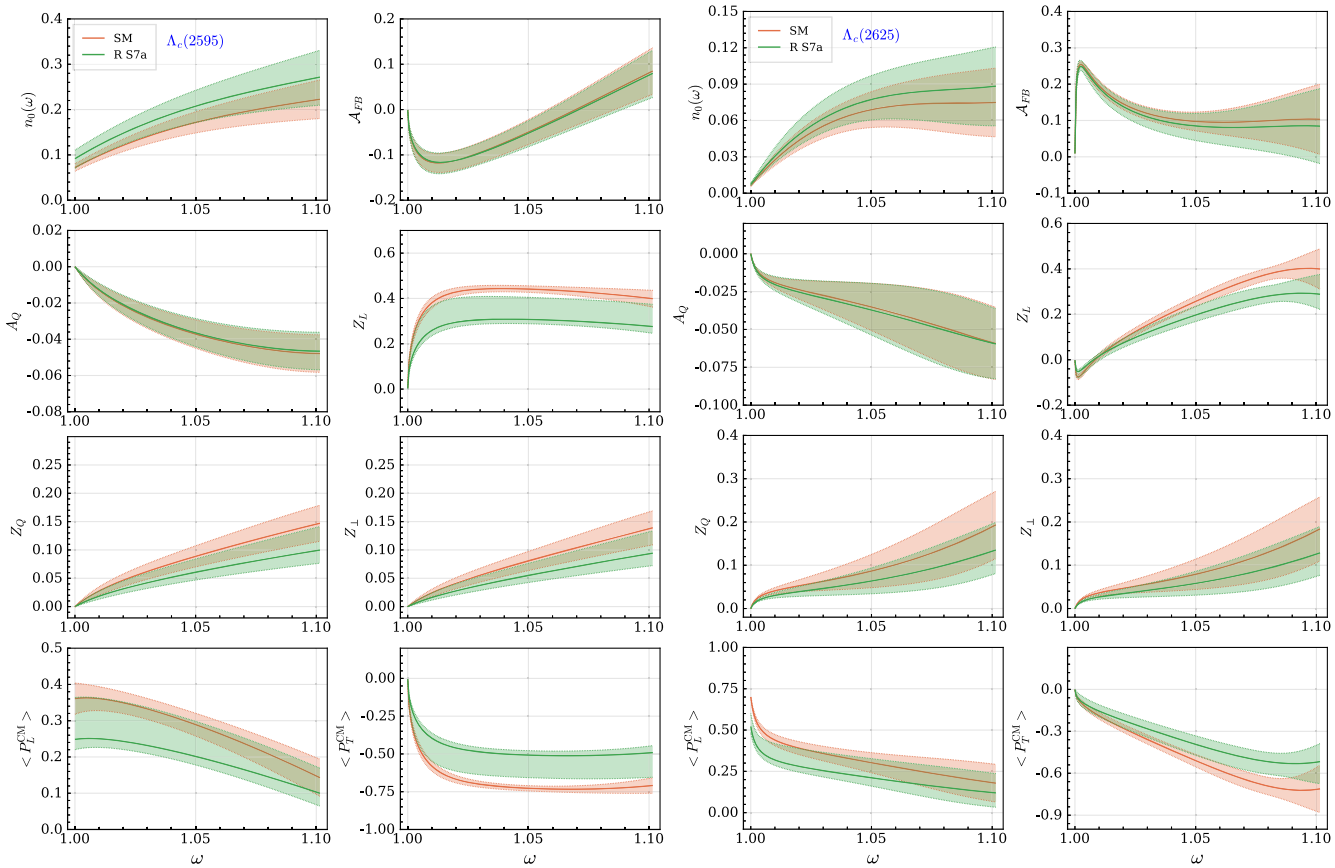

FIG. 3. Same as Figs. 1 and 2, but comparing in this case SM to the model corresponding to fit R S7a of Ref. [45], which NP contributions are constructed using right-handed neutrino fields. Two left columns: $\Lambda_b \to \Lambda_c^*(2595)\tau^-\bar{\nu}_\tau$ decay. Two right columns: $\Lambda_b \to \Lambda_c^*(2625)\tau^-\bar{\nu}_\tau$ decay.

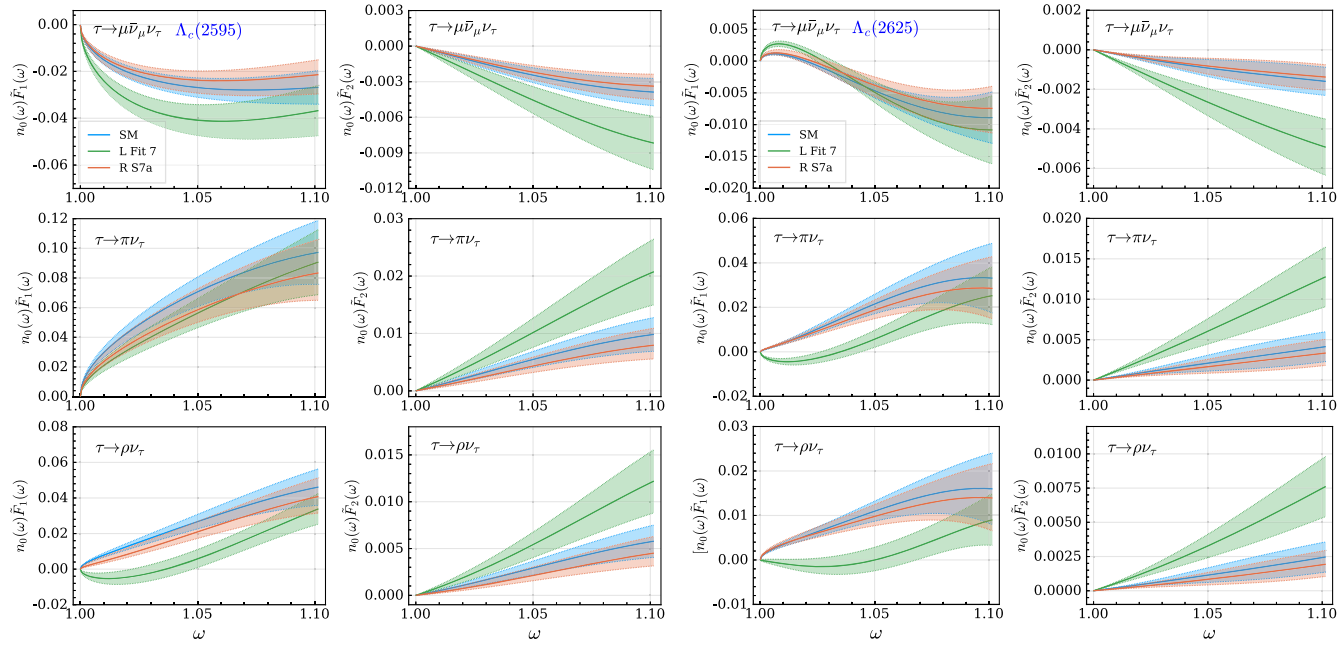

FIG. 4. Two left columns: $n_0(\omega)\widetilde{F}^d_{1,2}(\omega)$ for the three $\Lambda_b \to \Lambda_c^*(2595)\tau^-(\mu^-\bar{\nu}_\mu\nu_\tau, \pi^-\nu_\tau, \rho^-\nu_\tau)\bar{\nu}_\tau$ sequential decays evaluated within the SM, the L fit 7 model of Ref. [42] and the R S7a model of Ref. [45]. Two right columns: the same but for the $\Lambda_b \to \Lambda_c^*(2625)\tau^-(\mu^-\bar{\nu}_\mu\nu_\tau, \pi^-\nu_\tau, \rho^-\nu_\tau)\bar{\nu}_\tau$ sequential decays.

ones to be measured since they do not involve the second Legendre multipole in Eq. (15). We show results for both $\Lambda_b \to \Lambda_c^*(2595)$ and $\Lambda_b \to \Lambda_c^*(2625)$ semileptonic decays (panels in the first two and last two rows, respectively) and for the three beyond the SM scenarios considered in this work. In the left-handed neutrino NP models of fits 6 and 7 of Ref. [42], there is a total of five real WCs. In both cases (see Table I) the tensor coefficient $C^T_{\chi=L}$ is negligible, but even without considering the tensor contributions, we still have ten different contributions taking interference into account. In the plots collected in Fig. 5, we show SM and full results, as well as the predictions obtained when the SM is supplemented only by some of the NP terms.[7] For the sake of simplicity and clarity, we display only the largest contributions and eliminate the $\chi = L$ label. We do the same for the case of the right-handed neutrino R S7a scenario of Ref. [45], where always $C^V_{\chi=L} = C^A_{\chi=L} = 1$ and for the rest of WCs, the $\chi = R$ subindex is removed. Thus, for instance the curves denoted in Fig. 5 as C^S, both for L or R scenarios, stand for the results obtained when C^S is fixed to the corresponding value fitted in the NP scheme, and the other WCs are set to the SM values. Likewise, the $C^S + C^V$ lines show the predictions when C^S and C^V are fixed to the corresponding values fitted in the NP scheme, while the rest of the WCs are set to the SM values. In Fig. 5, we see that the main contributions responsible for the differences between the L fit 7 and SM predictions come from C^S and/or C^V. For the L fit 6, the latter are much smaller (see Table I), being closer to the SM values. This explains why the predictions from this NP scheme are more difficult to be distinguished from those obtained within the SM, cf. Figs. 1, 2, and 4. For the R S7a scheme, the main NP contributions originate from the right-handed neutrino C^A and C^V terms.

In Fig. 6, we present a similar analysis, but in this case for the visible pion-energy accumulated distributions $\widetilde{F}_1(\omega)$ and $\widetilde{F}_2(\omega)$ for the hadron $\tau^- \to \pi^-\nu_\tau$ decay mode. The last observable, $\widetilde{F}_2(\omega)$, depends on some of the asymmetries not considered in the previous figure. We do not show results from the L fit 6 of Ref. [42] since its predictions are similar to those obtained within the SM.

On the whole, we see that the observed pattern of changes induced by NP depend on the studied quantity and the information encoded in these two figures might be helpful to disentangle between different extensions of the SM.

Finally, we would like to stress that the expressions of the $\widetilde{W}_\chi$ SFs in terms of the $1/2^+ \to 1/2^-$ and $1/2^+ \to 3/2^-$ form factors derived in this work are general, and they do not apply only to the $\Lambda_b \to \Lambda_c^*(2595), \Lambda_c^*(2625)$ transitions studied here. Actually, using the appropriate numerical values for the form factors, these $\widetilde{W}_\chi$ SFs can be used for any $1/2^+ \to 1/2^-$ or $1/2^+ \to 3/2^-$ CC semileptonic decay, driven by a $q \to q'\ell^-\bar{\nu}_\ell$ transition at the quark level. This will allow to systematically analyze NP effects in the charged-lepton unpolarized and polarized differential distributions in all these kinds of reactions.

[7]Note that for $C^{V,A}_{\chi=L}$, NP is encoded in their deviations from one.

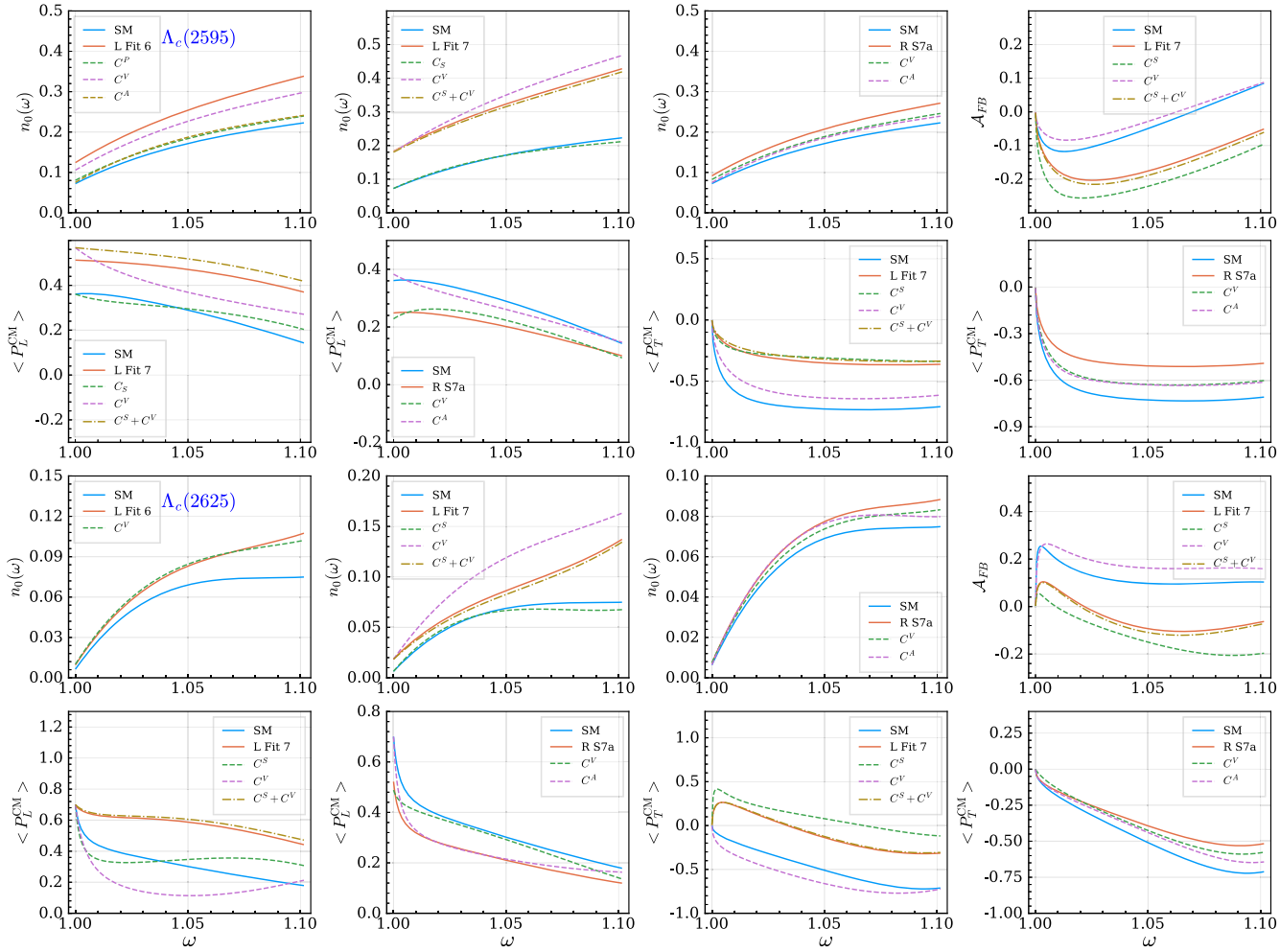

FIG. 5. SM, L fits 6 and 7 [42] and R S7a [45] results, as well as the predictions obtained when the SM is supplemented by only some of the NP terms (see text for details), for some selected observables among those which can be extracted from the visible differential decay width for the $H_b \to H_c \tau^-(\pi^- \nu_\tau)\bar{\nu}_\tau$ sequential decay [see Eq. (15)]. We show results for both the $\Lambda_b \to \Lambda_c^*(2595)$ (two top rows) and $\Lambda_b \to \Lambda_c^*(2625)$ (two bottom rows) semileptonic decays, and for the sake of clarity, we do not display uncertainty bands.

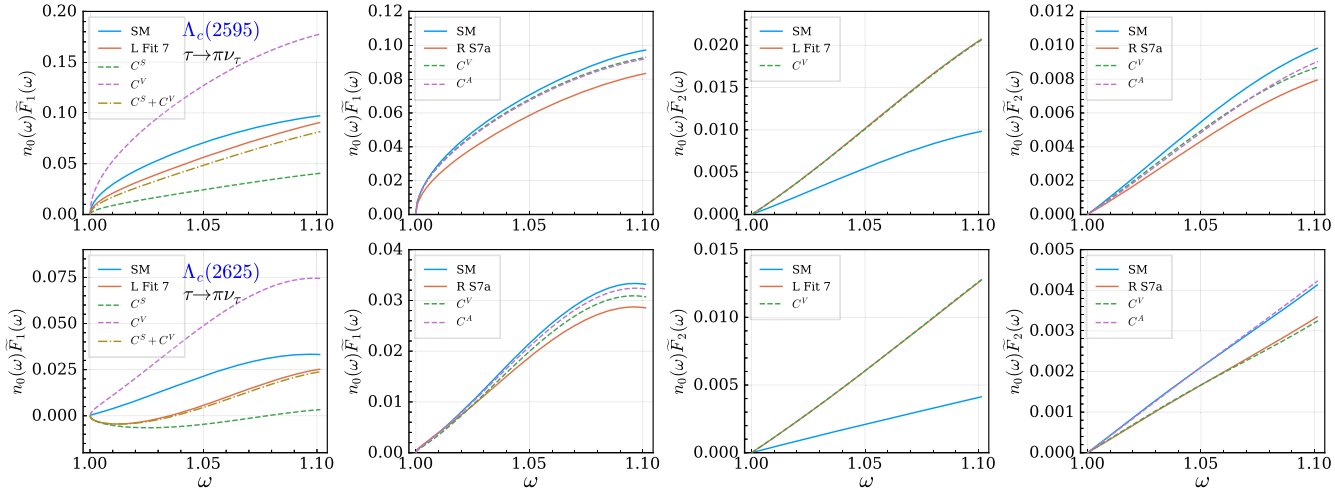

FIG. 6. Same as in Fig. 5, but for the pion-energy accumulated distributions $n_0(\omega)\widetilde{F}_1(\omega)$ and $n_0(\omega)\widetilde{F}_2(\omega)$. Here, we do not show results from the L fit 6 of Ref. [42].

ACKNOWLEDGMENTS

N. P. thanks Physics and Astronomy at the University of Southampton for hospitality while this work was completed and a Generalitat Valenciana Grant No. CIBEFP/2021/32. This research has been supported by the Spanish Ministerio de Ciencia e Innovación (MICINN) and the European Regional Development Fund (ERDF) under Contracts No. PID2020–112777 GB-I00 and No. PID2019–105439 GB-C22, the EU STRONG-2020 project under the Program H2020-INFRAIA-2018-1, Grant Agreement No. 824093 and by Generalitat Valenciana under Contract No. PROMETEO/2020/023.

APPENDIX A: HADRONIC MATRIX ELEMENTS AND SFs FOR $1/2^+ \to 1/2^-$ TRANSITIONS

1. Form factors

We parametrize the matrix elements of the different $b \to c$ transition operators for the $\Lambda_b \to \Lambda_c^*(2595)$ decay in such a way that we can make use of the expressions obtained in Refs. [65,71] for $1/2^+ \to 1/2^+$ transitions with a minimum of changes. To that end, we use the form factor decompositions[8]

$$\langle \Lambda_c^*; \vec{p}', r' | \bar{c}(0)\gamma^\alpha b(0) | \Lambda_b; \vec{p}, r\rangle = \bar{u}_{\Lambda_c^*,r'}(\vec{p}')\left(G_1\gamma^\alpha + G_2\frac{p^\alpha}{M} + G_3\frac{p'^\alpha}{M'}\right)\gamma_5 u_{\Lambda_b,r}(\vec{p}), \tag{A1}$$

$$\langle \Lambda_c^*; \vec{p}', r' | \bar{c}(0)\gamma^\alpha\gamma_5 b(0) | \Lambda_b; \vec{p}, r\rangle = \bar{u}_{\Lambda_c^*,r'}(\vec{p}')\left(F_1\gamma^\alpha + F_2\frac{p^\alpha}{M} + F_3\frac{p'^\alpha}{M'}\right) u_{\Lambda_b,r}(\vec{p}), \tag{A2}$$

$$\langle \Lambda_c^*; \vec{p}', r' | \bar{c}(0) b(0) | \Lambda_b; \vec{p}, r\rangle = F_P \bar{u}_{\Lambda_c^*,r'}(\vec{p}')\gamma_5 u_{\Lambda_b,r}(\vec{p}), \tag{A3}$$

$$\langle \Lambda_c^*; \vec{p}', r' | \bar{c}(0)\gamma_5 b(0) | \Lambda_b; \vec{p}, r\rangle = F_S \bar{u}_{\Lambda_c^*,r'}(\vec{p}') u_{\Lambda_b,r}(\vec{p}), \tag{A4}$$

$$\begin{aligned}\langle \Lambda_c^*; \vec{p}', r' | \bar{c}(0)\sigma^{\alpha\beta}\gamma_5 b(0) | \Lambda_b; \vec{p}, r\rangle = \bar{u}_{\Lambda_c^*,r'}(\vec{p}')\Big[& i\frac{T_1}{M^2}(p^\alpha p'^\beta - p^\beta p'^\alpha) + i\frac{T_2}{M}(\gamma^\alpha p^\beta - \gamma^\beta p^\alpha) \\ & + i\frac{T_3}{M}(\gamma^\alpha p'^\beta - \gamma^\beta p'^\alpha) + T_4\sigma^{\alpha\beta}\Big] u_{\Lambda_b,r}(\vec{p})\end{aligned} \tag{A5}$$

$$\langle \Lambda_c^*; \vec{p}', r' | \bar{c}(0)\sigma^{\alpha\beta} b(0) | \Lambda_b; \vec{p}, r\rangle = \bar{u}_{\Lambda_c^*,r'}(\vec{p}')\epsilon^{\alpha\beta}{}_{\rho\lambda}\left[\frac{T_1}{M^2}p^\rho p'^\lambda + \frac{T_2}{M}\gamma^\rho p^\lambda + \frac{T_3}{M}\gamma^\rho p'^\lambda + \frac{1}{2}T_4\gamma^\rho\gamma^\lambda\right] u_{\Lambda_b,r}(\vec{p}), \tag{A6}$$

where p and p' (M and M') are the four-momenta (masses) of the Λ_b and Λ_c^* baryons, respectively, $u_{\Lambda_b,\Lambda_c^*}$ are Dirac spinors, and we have made use of $\sigma^{\alpha\beta}\gamma_5 = -\frac{i}{2}\epsilon^{\alpha\beta}{}_{\rho\lambda}\sigma^{\rho\lambda}$. The form factors are Lorentz scalar functions of q^2 or equivalently of ω, the product of the four-velocities of the initial and final hadrons.

The form factors used in this work are related to the helicity ones evaluated in the LQCD simulation of Refs. [73,74] by

$$\begin{aligned}
G_1 &= -f_\perp^{(\frac{1}{2}^-)} \\
G_2 &= M\left(f_0^{(\frac{1}{2}^-)}\frac{M+M'}{q^2} + f_+^{(\frac{1}{2}^-)}\frac{M-M'}{s_-}\left(1-\frac{M^2-M'^2}{q^2}\right) + f_\perp^{(\frac{1}{2}^-)}\frac{2M'}{s_-}\right) \\
G_3 &= M'\left(-f_0^{(\frac{1}{2}^-)}\frac{M+M'}{q^2} + f_+^{(\frac{1}{2}^-)}\frac{M-M'}{s_-}\left(1+\frac{M^2-M'^2}{q^2}\right) - f_\perp^{(\frac{1}{2}^-)}\frac{2M}{s_-}\right)
\end{aligned} \tag{A7}$$

$$\begin{aligned}
F_1 &= -g_\perp^{(\frac{1}{2}^-)} \\
F_2 &= M\left(-g_0^{(\frac{1}{2}^-)}\frac{M-M'}{q^2} - g_+^{(\frac{1}{2}^-)}\frac{M+M'}{s_+}\left(1-\frac{M^2-M'^2}{q^2}\right) + g_\perp^{(\frac{1}{2}^-)}\frac{2M'}{s_+}\right) \\
F_3 &= M'\left(g_0^{(\frac{1}{2}^-)}\frac{M-M'}{q^2} - g_+^{(\frac{1}{2}^-)}\frac{M+M'}{s_+}\left(1+\frac{M^2-M'^2}{q^2}\right) + g_\perp^{(\frac{1}{2}^-)}\frac{2M}{s_+}\right)
\end{aligned} \tag{A8}$$

[8]The form factors defined in this work are related to those in Ref. [76] by identifying $G_i = d_{V_i}$, $F_i = d_{A_i}$, $F_P = d_S$, $F_S = d_P$, and $T_i = d_{T_i}$.

$$
\begin{aligned}
T_1 &= \frac{2M^2}{s_+}\left[h_+^{(\frac{1}{2}^-)} - \tilde{h}_+^{(\frac{1}{2}^-)} - \frac{s_+(M-M')^2}{q^2 s_-}(h_\perp^{(\frac{1}{2}^-)} - h_+^{(\frac{1}{2}^-)}) + \frac{(M+M')^2}{q^2}(\tilde{h}_\perp^{(\frac{1}{2}^-)} - h_+^{(\frac{1}{2}^-)})\right] \\
T_2 &= -\frac{2Mq\cdot p'}{q^2 s_-}(h_\perp^{(\frac{1}{2}^-)} - h_+^{(\frac{1}{2}^-)})(M-M') + \frac{M}{q^2}(\tilde{h}_\perp^{(\frac{1}{2}^-)} - h_+^{(\frac{1}{2}^-)})(M+M') \\
T_3 &= \frac{2Mq\cdot p}{q^2 s_-}(h_\perp^{(\frac{1}{2}^-)} - h_+^{(\frac{1}{2}^-)})(M-M') - \frac{M}{q^2}(\tilde{h}_\perp^{(\frac{1}{2}^-)} - h_+^{(\frac{1}{2}^-)})(M+M') \\
T_4 &= h_+^{(\frac{1}{2}^-)},
\end{aligned} \tag{A9}
$$

where $s_\pm = (M \pm M')^2 - q^2 = 2p\cdot p' \pm 2MM' = 2MM'(\omega \pm 1)$. Finally, thanks to the equations of motion of the heavy quarks, one can relate F_P and F_S to the vector and axial form factors as

$$
\begin{aligned}
F_P &= \frac{1}{m_b - m_c}[-(M+M')G_1 + (M - M'\omega)G_2 + (M\omega - M')G_3], \\
F_S &= -\frac{1}{m_b + m_c}[(M-M')F_1 + (M - M'\omega)F_2 + (M\omega - M')F_3],
\end{aligned} \tag{A10}
$$

with m_b and m_c the masses of the b and c quarks respectively.

2. Hadron tensors and $\widetilde{W}_\chi$ SFs

In Eqs. (A1)–(A6), we have interchanged the form factor decomposition of the $\bar{c}(0)O^{(\alpha\beta)}b(0)$ and $\bar{c}(0)O^{(\alpha\beta)}\gamma_5 b(0)$ matrix elements, with $O^{(\alpha\beta)} = I, \gamma^\alpha, \sigma^{\alpha\beta}$, with respect to the ones used in Refs. [65,71] for the $1/2^+ \to 1/2^+$ case due to the opposite parity here of the final charmed baryon. In this way, when comparing the vector ($J^\alpha_{HVrr'}$), axial ($J^\alpha_{HArr'}$), scalar ($J_{HSrr'}$), pseudoscalar ($J_{HPrr'}$), tensor ($J^{\alpha\beta}_{HTrr'}$) and pseudotensor ($J^{\alpha\beta}_{HpTrr'}$) hadronic matrix elements here with those for the $1/2^+ \to 1/2^+$ transition, and apart from the obvious differences in the actual values of the form factors, we only have to implement the following changes:

$$
\begin{aligned}
J^\alpha_{Hrr'\chi} &= C^V_\chi J^\alpha_{HVrr'} + h_\chi C^A_\chi J^\alpha_{HArr'} \to C^V_\chi J^\alpha_{HArr'} + h_\chi C^A_\chi J^\alpha_{HVrr'} = h_\chi[C^A_\chi J^\alpha_{HVrr'} + h_\chi C^V_\chi J^\alpha_{HArr'}], \\
J_{Hrr'\chi} &= C^S_\chi J_{HSrr'} + h_\chi C^P_\chi J_{HPrr'} \to C^S_\chi J_{HPrr'} + h_\chi C^P_\chi J_{HSrr'} = h_\chi[C^P_\chi J_{HSrr'} + h_\chi C^S_\chi J_{HPrr'}], \\
J^{\alpha\beta}_{Hrr'\chi} &= C^T_\chi(J^{\alpha\beta}_{HTrr'} + h_\chi J^{\alpha\beta}_{HpTrr'}) \to C^T_\chi(J^{\alpha\beta}_{HpTrr'} + h_\chi J^{\alpha\beta}_{HTrr'}) = h_\chi[C^T_\chi(J^{\alpha\beta}_{HTrr'} + h_\chi J^{\alpha\beta}_{HpTrr'})].
\end{aligned} \tag{A11}
$$

Since there is no left-right interference for massless neutrinos and all hadronic tensors are quadratic in the WCs, the global factor h_χ is irrelevant and, to get the $\widetilde{W}_\chi$ SFs for the $1/2^+ \to 1/2^-$ decay, it suffices to do the changes

$$
C^V_\chi \leftrightarrow C^A_\chi, \qquad C^S_\chi \leftrightarrow C^P_\chi \tag{A12}
$$

in our original expressions of Appendix C of Ref. [71]. In addition, the genuine hadron $W^{VV,AA}_{i=1,2,4,5}$, $W^{VA}_{i=3}$, $W^T_{1,2,3,4,5}$, W_S, W_P, $W^{VS,AP}_{I1,I2}$, $W^{ST,PpT}_{I3}$ and $W^{VT,ApT}_{I4,I5,I6,I7}$ SFs, which are independent of the WCs, can be read out from Eqs. (E3)–(E5) of Ref. [65] obtained for the $\Lambda_b \to \Lambda_c$ ($1/2^+ \to 1/2^+$) transition.

APPENDIX B: HADRONIC MATRIX ELEMENTS FOR $1/2^+ \to 3/2^-$ TRANSITION

1. Form factors

For the $\Lambda_b \to \Lambda_c^*(2625)$ decay, we use the following form factor decompositions[9]:

$$
\langle \Lambda_c^*; \vec{p}', r'|\bar{c}(0)\gamma^\alpha b(0)|\Lambda_b; \vec{p}, r\rangle = \bar{u}^\mu_{\Lambda_c^*, r'}(\vec{p}')\left[\frac{F_1^V}{M}p_\mu\gamma^\alpha + \frac{F_2^V}{M^2}p_\mu p^\alpha + \frac{F_3^V}{MM'}p_\mu p'^\alpha + F_4^V g_\mu{}^\alpha\right]u_{\Lambda_b, r}(\vec{p}), \tag{B1}
$$

[9]The form factors below are related to those in Ref. [76] as $F_i^{V,A,T} = l_{V,A,T_i}$ and $F_{S,P}^{(3/2)} = l_{S,P}$.

$$\langle \Lambda_c^*;\vec{p}',r'|\bar{c}(0)\gamma^\alpha b(0)|\Lambda_b;\vec{p},r\rangle = \bar{u}^\mu_{\Lambda_c^*,r'}(\vec{p}')\left[\frac{F_1^A}{M}p_\mu\gamma^\alpha + \frac{F_2^A}{M^2}p_\mu p^\alpha + \frac{F_3^A}{MM'}p_\mu p'^\alpha + F_4^A g_\mu{}^\alpha\right]\gamma_5 u_{\Lambda_b,r}(\vec{p}), \tag{B2}$$

$$\langle \Lambda_c^*;\vec{p}',r'|\bar{c}(0)b(0)|\Lambda_b;\vec{p},r\rangle = \bar{u}^\mu_{\Lambda_c^*,r'}(\vec{p}')p_\mu\frac{F_S^{(3/2)}}{M}u_{\Lambda_b,r}(\vec{p}), \tag{B3}$$

$$\langle \Lambda_c^*;\vec{p}',r'|\bar{c}(0)\gamma_5 b(0)|\Lambda_b;\vec{p},r\rangle = \bar{u}^\mu_{\Lambda_c^*,r'}(\vec{p}')p_\mu\frac{F_P^{(3/2)}}{M}\gamma_5 u_{\Lambda_b,r}(\vec{p}), \tag{B4}$$

$$\begin{aligned}\langle \Lambda_c^*;\vec{p}',r'|\bar{c}(0)\sigma^{\alpha\beta} b(0)|\Lambda_b;\vec{p},r\rangle = \bar{u}^\mu_{\Lambda_c^*,r'}(\vec{p}')\Big[&i\frac{F_1^T}{M^3}p_\mu(p^\alpha p'^\beta - p^\beta p'^\alpha) + i\frac{F_2^T}{M^2}p_\mu(\gamma^\alpha p^\beta - \gamma^\beta p^\alpha) + i\frac{F_3^T}{M^2}p_\mu(\gamma^\alpha p'^\beta - \gamma^\beta p'^\alpha)\\ &+\frac{F_4^T}{M}p_\mu\sigma^{\alpha\beta} + iF_5^T(g_\mu{}^\alpha\gamma^\beta - g_\mu{}^\beta\gamma^\alpha) + i\frac{F_6^T}{M}(g_\mu{}^\alpha p^\beta - g_\mu{}^\beta p^\alpha)\\ &+ i\frac{F_7^T}{M}(g_\mu{}^\alpha p'^\beta - g_\mu{}^\beta p'^\alpha)\Big]u_{\Lambda_b,r}(\vec{p})\end{aligned} \tag{B5}$$

$$\begin{aligned}\langle \Lambda_c^*;\vec{p}',r'|\bar{c}(0)\sigma^{\alpha\beta}\gamma_5 b(0)|\Lambda_b;\vec{p},r\rangle = \bar{u}^\mu_{\Lambda_c^*,r'}(\vec{p}')\Big[&\frac{F_1^T}{M^3}p_\mu\epsilon^{\alpha\beta}{}_{\rho\lambda}p^\rho p'^\lambda + \frac{F_2^T}{M^2}p_\mu\epsilon^{\alpha\beta}{}_{\rho\lambda}\gamma^\rho p^\lambda + \frac{F_3^T}{M^2}p_\mu\epsilon^{\alpha\beta}{}_{\rho\lambda}\gamma^\rho p'^\lambda - i\frac{F_4^T}{M}p_\mu\frac{1}{2}\epsilon^{\alpha\beta}{}_{\rho\lambda}\sigma^{\rho\lambda}\\ &+F_5^T\epsilon^{\alpha\beta}{}_{\mu\lambda}\gamma^\lambda + \frac{F_6^T}{M}\epsilon^{\alpha\beta}{}_{\mu\lambda}p^\lambda + \frac{F_7^T}{M}\epsilon^{\alpha\beta}{}_{\mu\lambda}p'^\lambda\Big]u_{\Lambda_b,r}(\vec{p}).\end{aligned} \tag{B6}$$

Here, $u^\mu(\vec{p}')$ is the Rarita-Schwinger spinor satisfying $\not{p}'u^\mu(p') = M'u^\mu(p')$ and the orthogonality conditions $\gamma_\mu u^\mu(p') = p'_\mu u^\mu(p') = 0$. Using these relations, together with $\not{p}u(\vec{p}) = Mu(\vec{p})$ and the identity

$$\epsilon^{\alpha\mu\nu\lambda} = -\gamma_5(-i\sigma^{\alpha\mu}\sigma^{\nu\lambda} - ig^{\alpha\lambda}g^{\mu\nu} + ig^{\alpha\nu}g^{\mu\lambda} + g^{\alpha\nu}\sigma^{\mu\lambda} + g^{\mu\lambda}\sigma^{\alpha\nu} - g^{\alpha\lambda}\sigma^{\mu\nu} - g^{\mu\nu}\sigma^{\alpha\lambda}), \tag{B7}$$

one can rewrite Eq. (B6) as

$$\begin{aligned}\langle \Lambda_c^*;\vec{p}',r'|\bar{c}(0)\sigma^{\alpha\beta}\gamma_5 b(0)|\Lambda_b;\vec{p},r\rangle = \bar{u}^\mu_{\Lambda_c^*,r'}(\vec{p}')\gamma_5\Big[&-ip_\mu(p^\alpha p'^\beta - p^\beta p'^\alpha)\frac{F_1^T}{M^3} + ip_\mu(\gamma^\alpha p^\beta - \gamma^\beta p^\alpha)\frac{M'F_1^T - MF_2^T}{M^3}\\ &+ ip_\mu(\gamma^\alpha p'^\beta - \gamma^\beta p'^\alpha)\frac{F_1^T + F_3^T}{M^2}\\ &+ p_\mu\sigma^{\alpha\beta}\left[\frac{F_6^T}{M} - \frac{F_1^T}{M^3}(p\cdot p' + MM') + \frac{F_2^T}{M} - \frac{M'}{M^2}F_3^T + \frac{F_4^T}{M}\right]\\ &+ i(g_\mu{}^\alpha\gamma^\beta - g_\mu{}^\beta\gamma^\alpha)\left(F_5^T + F_6^T + \frac{M'}{M}F_7^T\right) - i(g_\mu{}^\alpha p^\beta - g_\mu{}^\beta p^\alpha)\frac{F_6^T}{M}\\ &+ i(g_\mu{}^\alpha p'^\beta - g_\mu{}^\beta p'^\alpha)\frac{F_7^T}{M}\Big]u_{\Lambda_b,r}(\vec{p})\end{aligned} \tag{B8}$$

which will be the form used in the rest of the Appendix.

The vector and axial form factors used in this work are related to the helicity ones computed in Refs. [73,74] via

$$\begin{aligned}F_1^V &= (f_\perp^{(\frac{3}{2}^-)} + f_{\perp'}^{(\frac{3}{2}^-)})\frac{MM'}{s_-},\\ F_2^V &= M^2\left[f_0^{(\frac{3}{2}^-)}\frac{M'}{s_+}\frac{(M-M')}{q^2} + f_+^{(\frac{3}{2}^-)}\frac{M'}{s_-}\frac{(M+M')[q^2-(M^2-M'^2)]}{q^2 s_+} - (f_\perp^{(\frac{3}{2}^-)} - f_{\perp'}^{(\frac{3}{2}^-)})\frac{2M'^2}{s_- s_+}\right]\\ F_3^V &= M'^2\left[-f_0^{(\frac{3}{2}^-)}\frac{M}{s_+}\frac{(M-M')}{q^2} + f_+^{(\frac{3}{2}^-)}\frac{M}{s_-}\frac{(M+M')[q^2+(M^2-M'^2)]}{q^2 s_+} - \left[f_\perp^{(\frac{3}{2}^-)} - f_{\perp'}^{(\frac{3}{2}^-)}\left(1-\frac{s_+}{MM'}\right)\right]\frac{2M^2}{s_- s_+}\right],\\ F_4^V &= f_{\perp'}^{(\frac{3}{2}^-)}.\end{aligned} \tag{B9}$$

$$
\begin{aligned}
F_1^A &= (g_\perp^{(\frac{3}{2}^-)} + g_{\perp'}^{(\frac{3}{2}^-)}) \frac{MM'}{s_+}, \\
F_2^A &= M^2 \left[-g_0^{(\frac{3}{2}^-)} \frac{M'}{s_-} \frac{(M+M')}{q^2} - g_+^{(\frac{3}{2}^-)} \frac{M'}{s_+} \frac{(M-M')[q^2-(M^2-M'^2)]}{q^2 s_-} - (g_\perp^{(\frac{3}{2}^-)} - g_{\perp'}^{(\frac{3}{2}^-)}) \frac{2M'^2}{s_- s_+} \right] \\
F_3^A &= M'^2 \left[g_0^{(\frac{3}{2}^-)} \frac{M}{s_-} \frac{(M+M')}{q^2} - g_+^{(\frac{3}{2}^-)} \frac{M}{s_+} \frac{(M-M')[q^2+(M^2-M'^2)]}{q^2 s_-} + \left[g_\perp^{(\frac{3}{2}^-)} - g_{\perp'}^{(\frac{3}{2}^-)} \left(1 + \frac{s_-}{MM'} \right) \right] \frac{2M^2}{s_- s_+} \right], \\
F_4^A &= g_{\perp'}^{(\frac{3}{2}^-)}.
\end{aligned} \tag{B10}
$$

Moreover, using the equations of motion, one can relate $F_S^{(3/2)}$ and $F_P^{(3/2)}$ to the vector and axial form factors through

$$
\begin{aligned}
F_S^{(3/2)} &= \frac{1}{m_b - m_c} [(M-M')F_1^V + (M-M'\omega)F_2^V + (M\omega - M')F_3^V + MF_4^V], \\
F_P^{(3/2)} &= -\frac{1}{m_b + m_c} [-(M+M')F_1^A + (M-M'\omega)F_2^A + (M\omega - M')F_3^A + MF_4^A].
\end{aligned} \tag{B11}
$$

In the case of the matrix elements of the tensor operators, although there are seven different structures of the tensor (or pseudotensor) form, one of them can be removed without any loss of generality. As shown in Ref. [84], there is a combination of these structures that does not enter the physical amplitude. The argument goes as follows. Let us consider the contraction of the matrix element $J^{\alpha\beta}_{HTrr'}(p,q)$ of the tensor operator $\bar{c}(0)\sigma^{\alpha\beta}b(0)$ with a general tensor $F_{\alpha\beta}$. One would then have

$$
J^{\alpha\beta}_{HTrr'}(p,q)F_{\alpha\beta} = J^{\alpha\beta}_{HTrr'}(p,q) g_\alpha{}^{\alpha'} g_\beta{}^{\beta'} F_{\alpha'\beta'} = J^{\alpha\beta}_{HTrr'}(p,q) g_{rr} \epsilon_r^{\alpha'*} \epsilon_{r\alpha} g_{ss} \epsilon_s^{\beta'*} \epsilon_{s\beta} F_{\alpha'\beta'}, \tag{B12}
$$

with $\epsilon_{r=0,\pm1}$ the usual polarization vectors of a vector particle with four-momentum q and invariant mass $\sqrt{q^2}$, $\epsilon_{r=t} = \frac{q}{\sqrt{q^2}}$ and $-g_{tt} = g_{00} = g_{\pm1\pm1} = -1$. Since $J^{\alpha\beta}_{HTrr'}(p,q)$ is antisymmetric in the α, β indexes, one has

$$
J^{\alpha\beta}_{HTrr'}(p,q)\epsilon_{r\alpha}\epsilon_{s\beta} = J^{\alpha\beta}_{HTrr'}(p,q)\frac{1}{2}(\epsilon_{r\alpha}\epsilon_{s\beta} - \epsilon_{r\beta}\epsilon_{s\alpha}) \tag{B13}
$$

and then only six different products that correspond to the values $(r,s) = \{(t,0),(t,-1),(t,+1),(0,-1),(0,+1),(-1,+1)\}$ could appear. One can find $\lambda_{1-7}(q)$ scalar functions such that the linear combination

$$
\begin{aligned}
\Lambda^{\alpha\beta}_{HTrr'}(p,q,\vec{\lambda}) = \bar{u}_{r'\mu}(\vec{p}') \Bigg[& \frac{\lambda_1}{M^3} p^\mu (p^\alpha p'^\beta - p^\beta p'^\alpha) + \frac{\lambda_2}{M^2} p^\mu (\gamma^\alpha p^\beta - \gamma^\beta p^\alpha) + \frac{\lambda_3}{M^2} p^\mu (\gamma^\alpha p'^\beta - \gamma^\beta p'^\alpha) \\
& - i\frac{\lambda_4}{M} p^\mu \sigma^{\alpha\beta} + \lambda_5 (g^{\mu\alpha}\gamma^\beta - g^{\mu\beta}\gamma^\alpha) + \frac{\lambda_6}{M}(g^{\mu\alpha}p^\beta - g^{\mu\beta}p^\alpha) + \frac{\lambda_7}{M}(g^{\mu\alpha}p'^\beta - g^{\mu\beta}p'^\alpha) \Bigg] u_r(\vec{p})
\end{aligned} \tag{B14}
$$

is orthogonal to the six $\frac{1}{2}(\epsilon_{r\alpha}\epsilon_{s\beta} - \epsilon_{r\beta}\epsilon_{s\alpha})$ antisymmetric tensors.[10] A choice of such functions is given in Ref. [84] as

$$
\vec{\lambda} = \Lambda \left(0, 0, \frac{M}{M'}, 1, (\omega+1), -1, -\frac{M}{M'} \right), \tag{B17}
$$

where Λ is an arbitrary scalar function of q^2. Thus, no physical observable changes if one modifies

[10]Using that

$$
\epsilon^{\mu\nu\alpha\beta}\epsilon_{0\alpha}\epsilon_{t\beta} = i(\epsilon^\mu_{+1}\epsilon^\nu_{-1} - \epsilon^\nu_{+1}\epsilon^\mu_{-1}), \tag{B15}
$$

$$
\epsilon^{\mu\nu\alpha\beta}\epsilon_{\pm1\alpha}\epsilon_{t\beta} = \pm i(\epsilon^\mu_{\pm1}\epsilon^\nu_0 - \epsilon^\nu_{\pm1}\epsilon^\mu_0), \tag{B16}
$$

it is enough to ask for the orthogonality of both $\Lambda^{\alpha\beta}_{HTrr'}$ and $\Lambda^{\alpha\beta}_{HpTrr'} = -\frac{i}{2}\epsilon^{\alpha\beta}{}_{\rho\lambda}\Lambda^{\rho\lambda}_{HTrr'}$ to the combinations $\epsilon_0\epsilon_t$ and $\epsilon_{\pm1}\epsilon_t$.

$$
\begin{aligned}
F_3^T &\to F_3^{T'} = F_3^T + \Lambda\frac{M}{M'},\\
F_4^T &\to F_4^{T'} = F_3^T + \Lambda,\\
F_5^T &\to F_5^{T'} = F_5^T + \Lambda(\omega+1),\\
F_6^T &\to F_6^{T'} = F_6^T - \Lambda,\\
F_7^T &\to F_7^{T'} = F_7^T - \Lambda\frac{M}{M'},
\end{aligned}
\tag{B18}
$$

and Λ can be chosen so as to cancel one of the above form factors. For simplicity we omit the prime in what follows and take $F_7^T = 0$. Then one has the following relations between the tensor form factors here and the ones defined and evaluated in the LQCD simulation of Refs. [73,74]:

$$
\begin{aligned}
F_1^T &= -\frac{2M^3M'}{s_+s_-}(h_+^{(\frac{3}{2}^-)} - \tilde{h}_+^{(\frac{3}{2}^-)}) - \frac{2M^3M'(M-M')^2}{s_+s_-q^2}\tilde{h}_\perp^{(\frac{3}{2}^-)} + \frac{2M^3(M-M')(M^2-MM'-q^2)}{s_+s_-q^2}\tilde{h}_{\perp'}^{(\frac{3}{2}^-)}\\
&\quad + \frac{2M^3M'(M+M')^2}{s_+s_-q^2}h_\perp^{(\frac{3}{2}^-)} + \frac{2M^3(M+M')(M^2+MM'-q^2)}{s_+s_-q^2}h_{\perp'}^{(\frac{3}{2}^-)},\\
F_2^T &= \frac{2M^2M'^2}{s_+s_-}\tilde{h}_+^{(\frac{3}{2}^-)} - \frac{M^2M'(M-M')(M^2-M'^2-q^2)}{s_+s_-q^2}(\tilde{h}_\perp^{(\frac{3}{2}^-)} - \tilde{h}_{\perp'}^{(\frac{3}{2}^-)}) + \frac{M^2M'(M+M')}{s_-q^2}(h_\perp^{(\frac{3}{2}^-)} + h_{\perp'}^{(\frac{3}{2}^-)}),\\
F_3^T &= -\frac{2M^3M'}{s_+s_-}\tilde{h}_+^{(\frac{3}{2}^-)} + \frac{M^2M'(M-M')(M^2-M'^2+q^2)}{s_+s_-q^2}\tilde{h}_\perp^{(\frac{3}{2}^-)}\\
&\quad - \frac{M(M-M')(M^2+M'^2-MM'-q^2)(M^2-M'^2+q^2)}{s_+s_-q^2}\tilde{h}_{\perp'}^{(\frac{3}{2}^-)} - \frac{M^2M'(M+M')}{s_-q^2}h_\perp^{(\frac{3}{2}^-)}\\
&\quad - \frac{M(M^3+M'^3-q^2(M+M'))}{s_-q^2}h_{\perp'}^{(\frac{3}{2}^-)},\\
F_4^T &= \frac{MM'}{s_+}\tilde{h}_+^{(\frac{3}{2}^-)} - \frac{M'(M+M')}{q^2}h_{\perp'}^{(\frac{3}{2}^-)} - \frac{M'(M-M')(M^2-M'^2+q^2)}{q^2s_+}\tilde{h}_{\perp'}^{(\frac{3}{2}^-)},\\
F_5^T &= -\frac{1}{2Mq^2}[h_{\perp'}^{(\frac{3}{2}^-)}(M+M')s_+ + \tilde{h}_{\perp'}^{(\frac{3}{2}^-)}(M-M')(M^2-M'^2+q^2)],\\
F_6^T &= \frac{1}{q^2}[h_{\perp'}^{(\frac{3}{2}^-)}(M+M')^2 + \tilde{h}_{\perp'}^{(\frac{3}{2}^-)}(M-M')^2].
\end{aligned}
\tag{B19}
$$

2. Hadron tensors and $\widetilde{W}_\chi$ SFs

As already mentioned, in Refs. [65,71] we derived general expressions for the hadronic tensors that are valid for any CC transition, the differences being encoded in the actual values of the $\widetilde{W}_\chi$ SFs. In this case, writing

$$
J^{\mu(\alpha\beta)}_{H\chi rr'} = \bar{u}_{r'\mu}(\vec{p}\,')\Gamma^{\mu(\alpha\beta)}_{H\chi}u_r(\vec{p}\,'),
\tag{B20}
$$

we have that the hadronic tensors are given by the traces

$$
W_\chi^{(\alpha\beta)(\rho\lambda))} = \frac{1}{2}\mathrm{Tr}\left[\left(\sum_{r'}u_{r'\nu}(\vec{p}\,')\bar{u}_{r'\mu}(\vec{p}\,')\right)\Gamma^{\mu(\alpha\beta)}_{H\chi}\left(\sum_r u_r(\vec{p})\bar{u}_r(\vec{p})\right)\gamma^0\Gamma^{\nu(\rho\lambda)\dagger}_{H\chi}\gamma^0\right],
\tag{B21}
$$

with

$$
\sum_r u_r(\vec{p})\bar{u}_r(\vec{p}) = (\not{p}+M),
\tag{B22}
$$

$$
\sum_{r'}u_{r'\nu}(\vec{p}\,')\bar{u}_{r'\mu}(\vec{p}\,') = -(\not{p}'+M')\left[g_{\nu\mu} - \frac{1}{3}\gamma_\nu\gamma_\mu - \frac{2}{3}\frac{p'_\nu p'_\mu}{M'^2} + \frac{1}{3}\frac{p'_\nu\gamma_\mu - p'_\mu\gamma_\nu}{M'}\right]
\tag{B23}
$$

and

$$\Gamma_{H\chi}^{\mu(\alpha\beta)} = C_\chi^V \Gamma_{HV}^{\mu\alpha} + h_\chi C_\chi^A \Gamma_{HA}^{\mu\alpha}, \qquad C_\chi^S \Gamma_{HS}^{\mu} + h_\chi C_\chi^P \Gamma_{HP}^{\mu}, \qquad C_\chi^T (\Gamma_{HT}^{\mu\alpha\beta} + h_\chi \Gamma_{HpT}^{\mu\alpha\beta}), \tag{B24}$$

where the Γ's can be easily read out from Eqs. (B1)–(B6).

From a direct comparison of the results for those traces with the general form of the different $W_\chi^{(\alpha\beta)(\rho\lambda)}$ tensors in Refs. [65,71] we extract the corresponding $1/2^+ \to 3/2^-$ $\widetilde{W}_\chi$ SFs. They have been obtained with the use of the FeynCalc package [85–87] on *Mathematica* [88] and they are given in terms of the WCs and form factors by the following expressions[11]:

$$\begin{aligned}\widetilde{W}_{1\chi} = \frac{1}{3}\{&|C_\chi^V|^2(\omega+1)[(F_4^V)^2 + (F_1^V)^2(\omega-1)^2 - F_1^V F_4^V(\omega-1)] \\ &+ |C_\chi^A|^2(\omega-1)[(G_4^V)^2 + (G_1^V)^2(\omega+1)^2 - G_1^V G_4^V(\omega+1)]\},\end{aligned} \tag{B25}$$

$$\begin{aligned}\widetilde{W}_{2\chi} = \frac{1}{3M'^2}\{&|C_\chi^V|^2[2(F_1^V)^2 MM'(\omega^2-1) + F_1^V[F_4^V(M^2(1+2\omega) - 2MM' - M'^2) \\ &+ 2(M+M')(\omega^2-1)(F_3^V M + F_2^V M')] + (\omega+1)[(F_4^V)^2 M^2 \\ &- 2(F_3^V M + F_2^V M')F_4^V(M' - M\omega) + (\omega^2-1)(F_3^V M + F_2^V M')^2]] \\ &+ |C_\chi^A|^2[2(F_1^A)^2 MM'(\omega^2-1) + F_1^A[F_4^A(M^2(1-2\omega) + 2MM' - M'^2) \\ &- 2(M-M')(\omega^2-1)(F_3^A M + F_2^A M')] + (\omega-1)[(F_4^A)^2 M^2 \\ &- 2(F_3^A M + F_2^A M')F_4^A(M' - M\omega) + (\omega^2-1)(F_3^A M + F_2^A M')^2]]\},\end{aligned} \tag{B26}$$

$$\widetilde{W}_{3\chi} = -\frac{2\mathrm{Re}(C_\chi^V C_\chi^{A*})M}{3M'}\{F_4^V[F_1^A(\omega+1) + F_4^A] + (\omega-1)F_1^V[F_4^A - 2F_1^A(\omega+1)]\}, \tag{B27}$$

$$\begin{aligned}\widetilde{W}_{4\chi} = \frac{M^2}{3M'^2}\{&|C_\chi^V|^2[F_1^V[F_4^V(1+2\omega) + 2F_3^V(\omega^2-1)] + (\omega+1)[(F_4^V)^2 + 2F_3^V F_4^V \omega + (F_3^V)^2(\omega^2-1)]] \\ &+ |C_\chi^A|^2[F_1^A[F_4^A(1-2\omega) - 2F_3^A(\omega^2-1)] + (\omega-1)[(F_4^A)^2 + 2F_3^A F_4^A \omega + (F_3^A)^2(\omega^2-1)]]\},\end{aligned} \tag{B28}$$

$$\begin{aligned}\widetilde{W}_{5\chi} = \frac{2M}{3M'}\{&|C_\chi^V|^2[-(\omega^2-1)[(F_1^V + F_2^V)(F_1^V + F_3^V) + F_2^V F_3^V \omega] + F_4^V[F_1^V + (F_3^V - F_2^V\omega)(\omega+1)] \\ &- \frac{M}{M'}\{F_1^V[2F_3^V(\omega^2-1) + F_4^V(1+2\omega)] + (\omega+1)[(F_4^V)^2 + 2F_3^V F_4^V \omega + (F_3^V)^2(\omega^2-1)]\}] \\ &+ |C_\chi^A|^2[-(\omega^2-1)[(F_1^A - F_2^A)(F_1^A + F_3^A) + F_2^A F_3^A \omega] - F_4^A[F_1^A - (F_3^A - F_2^A\omega)(\omega-1)] \\ &+ \frac{M}{M'}\{F_1^A[2F_3^A(\omega^2-1) + F_4^A(2\omega-1)] - (\omega-1)[(F_4^A)^2 + 2F_3^A F_4^A \omega + (F_3^A)^2(\omega^2-1)]\}]\},\end{aligned} \tag{B29}$$

$$\widetilde{W}_{SP\chi} = \frac{\omega^2-1}{3}[|C_\chi^S|^2 (F_S^{(3/2)})^2(\omega+1) + |C_\chi^P|^2 (F_P^{(3/2)})^2(\omega-1)], \tag{B30}$$

$$\begin{aligned}\widetilde{W}_{I1\chi} = \frac{2}{3M'}\{&C_\chi^V C_\chi^{S*} F_S^{(3/2)}(\omega+1)[F_1^V(M+M')(\omega-1) + (F_2^V M' + F_3^V M)(\omega^2-1) \\ &+ F_4^V(M\omega - M')] + C_\chi^A C_\chi^{P*} F_P^{(3/2)}(\omega-1)[F_1^A(M'-M)(\omega+1) \\ &+ (F_2^A M' + F_3^A M)(\omega^2-1) + F_4^A(M\omega - M')]\},\end{aligned} \tag{B31}$$

$$\begin{aligned}\widetilde{W}_{I2\chi} = \frac{2M}{3M'}\{&-C_\chi^V C_\chi^{S*} F_S^{(3/2)}(\omega+1)[F_1^V(\omega-1) + F_3^V(\omega^2-1) + F_4^V\omega] \\ &+ C_\chi^A C_\chi^{P*} F_P^{(3/2)}(\omega-1)[F_1^A(\omega+1) - F_3^A(\omega^2-1) - F_4^A\omega]\},\end{aligned} \tag{B32}$$

$$\begin{aligned}\widetilde{W}_{I3\chi} = -\frac{2}{3M'}\{&C_\chi^S C_\chi^{T*} F_S^{(3/2)}(\omega+1)[M[F_5^T + \omega F_6^T + (F_2^T + F_4^T)(\omega-1)] \\ &+ M'[F_7^T - (\omega-1)(F_1^T(\omega+1) + F_3^T)]] \\ &+ C_\chi^P C_\chi^{T*} F_P^{(3/2)}(\omega-1)M[-F_5^T + F_4^T(\omega+1)]\},\end{aligned} \tag{B33}$$

[11]Here we have kept the explicit dependence on F_7^T.

$$\widetilde{W}_{I4\chi} = \frac{1}{3M'^2}\{C_\chi^V C_\chi^{T*}[-F_1^V\{F_5^T M(M'+M(2\omega+1)) + F_6^T M(M'\omega + M(2\omega+1)) + M'[(2MF_2^T - 2MF_3^T - 2(M+M')F_1^T)(\omega^2-1) + F_7^T(M(2+\omega)+M')]\} - 2(F_2^V M' + F_3^V M)(\omega+1) \times \{-F_1^T M'(\omega^2-1) + [M(F_2^T+F_4^T) - M'F_3^T](\omega-1) + M(F_5^T + F_6^T\omega) + M'F_7^T\} - F_4^V\{2F_1^T M'(\omega+1)[M'-M\omega] + F_2^T M[M(1+2\omega) - M'(2+\omega)] + F_3^T M'(M'-M\omega) + F_4^T M[M(1+2\omega) - M'] + M^2[F_5^T + 2F_6^T(\omega+1)]\}] + C_\chi^A C_\chi^{T*} M[F_1^A\{M'(\omega+1)[-2(F_2^T+F_3^T)(\omega-1) + F_6^T + F_7^T] + F_5^T(M' + M(2\omega-1))\} - 2(F_2^A M' + F_3^A M)(\omega-1)[F_4^T(\omega+1) - F_5^T] + F_4^A\{MF_5^T + M'[F_6^T + F_7^T + (\omega-1)(F_2^T+F_3^T)] + F_4(M(1-2\omega)+M')\}]\}, \tag{B34}$$

$$\widetilde{W}_{I5\chi} = \frac{M}{3M'^2}\{C_\chi^V C_\chi^{T*}[F_1^V\{(F_5^T+F_6^T)M(1+2\omega) + M'[F_7^T(\omega+2) - 2(F_1^T+F_3^T)(\omega^2-1)]\} + 2F_3^V(\omega+1)\{M'[-F_1^T(\omega^2-1) - F_3^T(\omega-1) + F_7^T] + M[F_5^T + (F_2^T+F_4^T)(\omega-1) + F_6^T\omega]\} + F_4^V\{-M'[2F_1^T\omega(\omega+1) + F_3^T\omega] + M[F_5^T + 2F_6^T(1+\omega) + (F_2^T+F_4^T)(1+2\omega)]\}] + C_\chi^A C_\chi^{T*}[-F_1^A\{F_5^T M(2\omega-1) + M'(\omega+1)[-2F_3^T(\omega-1) + F_7^T]\} + 2F_3^A M(\omega-1)[F_4^T(\omega+1) - F_5^T] - F_4^A\{F_5^T M + M'[F_3^T(\omega-1) + F_7^T] + F_4^T M(1-2\omega)\}]\}, \tag{B35}$$

$$\widetilde{W}_{I6\chi} = \frac{1}{3MM'}\{C_\chi^V C_\chi^{T*} M[F_1^V(\omega-1)\{F_5^T[M' - M(1+2\omega)] + (\omega+1)[2F_4^T(M-M') - M'[-2(F_2^T+F_3^T)(\omega-1) + F_6^T + F_7^T]]\} + F_4^V\{(\omega+1)[F_4^T(M'-M) + M'[(F_2^T+F_3^T)(1-\omega) + 2(F_6^T+F_7^T)]] + F_5^T[M' + M(2+\omega)]\}] - C_\chi^A C_\chi^{T*}[F_1^A(\omega+1)\{2F_2^T M(\omega-1)(M-M'\omega) + 2F_3^T M'(\omega-1)(M\omega - M') + 2F_4^T M(M+M')(\omega-1) + F_5^T M[M' + M(1-2\omega)] - F_6^T M(M-M'\omega) + F_7^T M'(M'-M\omega)\} + F_4^A\{-F_2^T M(\omega-1)(M-M'\omega) + F_3^T M'(\omega-1)(M'-M\omega) - F_4^T M(M+M')(\omega-1) + F_5^T M[M' + M(\omega-2)] - F_6^T M(M-M'\omega) + F_7^T M'(M'-M\omega)\}]\}, \tag{B36}$$

$$\widetilde{W}_{I7\chi} = \frac{1}{3M'}\{-C_\chi^V C_\chi^{T*}[F_1^V(\omega-1)\{(\omega+1)[2F_4^T M - M'[F_7^T - 2F_3^T(\omega-1)]] - F_5^T M(1+2\omega)\} + F_4^V\{(\omega+1)[-F_4^T M + M'[2F_7^T - F_3^T(\omega-1)]] + F_5^T M(2+\omega)\}] + C_\chi^A C_\chi^{T*}[F_1^A(\omega+1)\{2[(F_2^T+F_4^T)M + F_3^T M'\omega](\omega-1) + F_5^T M(1-2\omega) - F_6^T M - F_7^T M'\omega\} - F_4^A\{[(F_2^T+F_4^T)M + F_3^T M'\omega](\omega-1) + F_5^T M(2-\omega) + F_6^T M + F_7^T M'\omega\}]\}, \tag{B37}$$

$$\widetilde{W}_{1\chi}^T = \frac{|C_\chi^T|^2}{3M^2}\{M^2[2\omega(F_5^T)^2 + 2(\omega+1)F_5^T(F_6^T\omega + F_2^T(\omega-1)) + (\omega+1)[\omega^2((F_4^T)^2 + (F_6^T+F_2^T+F_4^T)^2) - 2\omega(F_2^T+F_4^T)(F_6^T+F_2^T+F_4^T) + F_2^T(F_2^T+2F_4^T)]] + 2MM'(\omega+1)[F_5^T + \omega F_6^T - (F_2^T+F_4^T)(1-\omega)][F_7^T - (\omega-1)(F_1^T(1+\omega)+F_3^T)] + M'^2(\omega+1)[F_7^T - (\omega-1)(F_1^T(1+\omega)+F_3^T)]^2\}, \tag{B38}$$

$$\widetilde{W}_{3\chi}^T = \frac{|C_\chi^T|^2}{3M'^2}\{M^2[-2\omega(F_5^T)^2 + F_5^T(F_6^T + F_2^T(1+2\omega) + 4\omega F_4^T) + F_6^T[F_6^T(1+\omega) + (F_2^T+F_4^T)(1+2\omega)]] + MM'[-2\omega^2[F_6^T F_1^T + F_2^T(F_1^T+F_3^T) + F_4^T(F_1^T+2F_3^T)] - \omega F_6^T(2F_1^T+F_3^T) + 2F_2^T(F_1^T+F_3^T) + 2F_4^T(F_1^T+2F_3^T) + F_5^T[-2F_7^T(2+\omega) - 2F_1^T(1+\omega) - F_3^T(3+2\omega-4\omega^2)] + F_7^T[F_2^T(\omega+2) + F_4^T(2\omega+3)]] - M'^2[2(\omega+1)(F_7^T)^2 + F_7^T[2(\omega+1)F_1^T + F_3^T(3-2\omega^2)] - (\omega^2-1)[(\omega+1)(F_1^T)^2 + 2F_1^T F_3^T - 2(\omega-1)(F_3^T)^2]]\}, \tag{B39}$$

$$\begin{aligned}\widetilde{W}_{2\chi}^T = &-\frac{|C_\chi^T|^2}{3M^2M'^2}\{M^4[2\omega(F_5^T)^2 - F_5^T(F_6^T + F_2^T(1+2\omega) + 4\omega F_4^T) - F_6^T[F_6^T(1+\omega)\\ &+ (F_2^T + F_4^T)(1+2\omega)]] + M^3M'[2(F_5^T)^2 - 4(F_4^T)^2 + F_5^T[4F_6^T(\omega+1)\\ &+ 2F_7^T(2+\omega) + 2F_1^T(1+\omega) + 2F_2^T(1+2\omega) + F_3^T(3+2\omega-4\omega^2) + 4F_4^T]\\ &+ 2\omega^2[(F_6^T)^2 + F_6^T(F_1^T + 2(F_2^T + F_4^T)) + 2(F_4^T)^2 + F_2^T(F_1^T + F_3^T)\\ &+ F_4^T(F_1^T + 2(F_2^T + F_3^T))] - 2F_2^T(F_1^T + F_3^T) - 2F_4^T(F_6^T + F_1^T + 2(F_2^T + F_3^T))\\ &+ \omega F_6^T(2(F_6^T + F_1^T + F_2^T) + F_3^T) - F_7^T[(\omega+2)F_2^T + F_4^T(2\omega+3)]]\\ &+ M^2M'^2[-\omega^3[(F_1^T)^2 + 4F_1^T(F_6^T + F_2^T + F_4^T) - 2((F_2^T)^2 + (F_3^T)^2)]\\ &- \omega^2[(F_1^T)^2 + 2F_1^T(2F_5^T + F_3^T) + 2((F_2^T)^2 + (F_3^T)^2) + 2F_3^T(F_7^T + 2F_2^T)\\ &+ 2F_6^T(2F_1^T + F_2^T + 2F_3^T) + 4F_4^T(F_2^T + F_3^T)]\\ &+ \omega[(F_6^T)^2 + 2F_6^T(2F_7^T - F_2^T) + 2((F_7^T)^2 - (F_2^T)^2 - (F_3^T)^2) + (F_1^T)^2\\ &+ 2F_1^T(-2F_5^T + F_7^T + 2F_2^T) + 4F_7^TF_2^T + 4F_4^T(F_7^T + F_1^T)]\\ &+ (F_6^T)^2 + (F_1^T)^2 + 2((F_7^T)^2 + (F_2^T)^2 + (F_3^T)^2)\\ &+ F_5^T(F_6^T + 2F_7^T - 3F_2^T - 2F_3^T) + F_6^T(4F_7^T + F_2^T + 2F_3^T + F_4^T)\\ &+ F_7^T(2F_1^T + 2F_2^T + 3F_3^T + 2F_4^T) + 2F_3^T(F_1^T + 2F_2^T) + 4F_4^T(F_2^T + F_3^T)]\\ &+ MM'^3[2F_2^TF_3^T\omega^2 + 2(F_1^T)^2\omega(\omega-1)(\omega+1)^2 + \omega(-F_7^TF_2^T + F_6^TF_3^T\\ &- 2F_7^TF_3^T) - 2F_2^TF_3^T - F_7^T(2F_2^T + F_4^T) + F_5^T(F_3^T + 2F_1^T(\omega+1))\\ &+ 2(\omega+1)F_1^T[(\omega-1)(F_2^T + F_4^T) + \omega(F_6^T - 2(F_7^T - F_3^T(\omega-1)))]]\\ &+ M'^4[F_7^T(F_3^T + 2F_1^T(\omega+1)) - (\omega^2-1)F_1^T(F_1^T(\omega+1) + 2F_3^T)]\},\end{aligned} \tag{B40}$$

$$\begin{aligned}\widetilde{W}_{4\chi}^T = &\frac{|C_\chi^T|^2}{3MM'^2}\{M^3[2\omega(F_5^T)^2 - F_5^T(F_6^T + F_2^T(1+2\omega) + 4\omega F_4^T) - F_6^T[F_6^T(1+\omega)\\ &+ (F_2^T + F_4^T)(1+2\omega)]] + M^2M'[(F_5^T)^2 + F_5^T[-4F_3^T\omega^2 + 2\omega(F_6^T + F_7^T + F_1^T + F_2^T + F_3^T)\\ &+ 2F_6^T + 4F_7^T + 2F_1^T + F_2^T + 3F_3^T + 2F_4^T] + \omega^2[(F_6^T)^2 + 2F_6^T(F_1^T + F_2^T + F_4^T)]\\ &+ 2(\omega^2-1)[(F_4^T)^2 + F_4^T(F_1^T + F_2^T + 2F_3^T) + F_2^T(F_1^T + F_3^T)] + \omega F_6^T(2F_1^T + F_2^T + F_3^T) + F_6^T(\omega F_6^T - F_4^T)\\ &- F_7^T[(\omega+2)F_2^T + (2\omega+3)F_4^T]] + MM'^2[-\omega^3[F_1^T(F_1^T + 2(F_6^T + F_2^T + F_4^T))\\ &- 2(F_3^T)^2] - \omega^2[2F_5^TF_1^T + 2F_6^T(F_1^T + F_3^T) + 2F_7^TF_3^T + F_1^T(F_1^T + 2F_3^T)\\ &+ 2F_3^T(F_2^T + F_3^T + F_4^T)] + \omega[2F_7^T(F_6^T + F_7^T + F_1^T + F_2^T + F_4^T) - 2(F_3^T)^2\\ &+ F_1^T(-2F_5^T + F_1^T + 2(F_2^T + F_4^T))] + F_7^T(2F_7^T + F_5^T + 2F_6^T + 2F_1^T + F_2^T\\ &+ 3F_3^T + F_4^T) + F_1^T(F_1^T + 2F_3^T) + F_3^T(2F_3^T - F_5^T + F_6^T + 2F_2^T + 2F_4^T)]\\ &+ M'^3\omega[(\omega^2-1)F_1^T(F_1^T(\omega+1) + 2F_3^T) - F_7^T(F_3^T + 2F_1^T(\omega+1))]\}.\end{aligned} \tag{B41}$$

As shown in Refs. [65,71], one has the general constraint

$$2M^2\widetilde{W}_{1\chi}^T + p^2\widetilde{W}_{2\chi}^T + q^2\widetilde{W}_{3\chi}^T + 2p\cdot q\widetilde{W}_{4\chi}^T = 0, \tag{B42}$$

which allows to eliminate $\widetilde{W}_{1\chi}^T$ in terms of the other three SFs. In fact, as shown in Refs. [65,71], the term in $\widetilde{W}_{1\chi}^T$ of the hadron tensor does not contribute when contracted with the corresponding lepton tensor.

[1] G. Aad *et al.* (ATLAS Collaboration), Phys. Lett. B **716**, 1 (2012).
[2] S. Chatrchyan *et al.* (CMS Collaboration), Phys. Lett. B **716**, 30 (2012).
[3] P. Langacker, *The Standard Model and Beyond* (CRC Press, Taylor & Francis, Boca Raton, FL, 2017).
[4] J. P. Lees *et al.* (*BABAR* Collaboration), Phys. Rev. Lett. **109**, 101802 (2012).
[5] J. P. Lees *et al.* (*BABAR* Collaboration), Phys. Rev. D **88**, 072012 (2013).
[6] M. Huschle *et al.* (Belle Collaboration), Phys. Rev. D **92**, 072014 (2015).
[7] Y. Sato *et al.* (Belle Collaboration), Phys. Rev. D **94**, 072007 (2016).
[8] S. Hirose *et al.* (Belle Collaboration), Phys. Rev. Lett. **118**, 211801 (2017).
[9] G. Caria *et al.* (Belle Collaboration), Phys. Rev. Lett. **124**, 161803 (2020).
[10] R. Aaij *et al.* (LHCb Collaboration), Phys. Rev. Lett. **115**, 111803 (2015); **115**, 159901(E) (2015).
[11] R. Aaij *et al.* (LHCb Collaboration), Phys. Rev. Lett. **120**, 171802 (2018).
[12] R. Aaij *et al.* (LHCb Collaboration), Phys. Rev. D **97**, 072013 (2018).
[13] Y. S. Amhis *et al.* (HFLAV Collaboration), Eur. Phys. J. C **81**, 226 (2021).
[14] R. Aaij *et al.* (LHCb Collaboration), Phys. Rev. Lett. **120**, 121801 (2018).
[15] A. Y. Anisimov, I. M. Narodetsky, C. Semay, and B. Silvestre-Brac, Phys. Lett. B **452**, 129 (1999).
[16] M. A. Ivanov, J. G. Korner, and P. Santorelli, Phys. Rev. D **73**, 054024 (2006).
[17] E. Hernández, J. Nieves, and J. Verde-Velasco, Phys. Rev. D **74**, 074008 (2006).
[18] T. Huang and F. Zuo, Eur. Phys. J. C **51**, 833 (2007).
[19] W. Wang, Y.-L. Shen, and C.-D. Lu, Phys. Rev. D **79**, 054012 (2009).
[20] W.-F. Wang, Y.-Y. Fan, and Z.-J. Xiao, Chin. Phys. C **37**, 093102 (2013).
[21] R. Watanabe, Phys. Lett. B **776**, 5 (2018).
[22] A. Issadykov and M. A. Ivanov, Phys. Lett. B **783**, 178 (2018).
[23] C.-T. Tran, M. A. Ivanov, J. G. Körner, and P. Santorelli, Phys. Rev. D **97**, 054014 (2018).
[24] X.-Q. Hu, S.-P. Jin, and Z.-J. Xiao, Chin. Phys. C **44**, 023104 (2020).
[25] D. Leljak, B. Melic, and M. Patra, J. High Energy Phys. 05 (2019) 094.
[26] K. Azizi, Y. Sarac, and H. Sundu, Phys. Rev. D **99**, 113004 (2019).
[27] W. Wang and R. Zhu, Int. J. Mod. Phys. A **34**, 1950195 (2019).
[28] S. Fajfer, J. F. Kamenik, and I. Nisandzic, Phys. Rev. D **85**, 094025 (2012).
[29] A. Abdesselam *et al.* (Belle Collaboration), in *Proceedings of the 10th International Workshop on the CKM Unitarity Triangle* (2019), arXiv:1903.03102.
[30] R. Alonso, B. Grinstein, and J. Martin Camalich, Phys. Rev. Lett. **118**, 081802 (2017).
[31] U. Nierste, S. Trine, and S. Westhoff, Phys. Rev. D **78**, 015006 (2008).
[32] M. Tanaka and R. Watanabe, Phys. Rev. D **87**, 034028 (2013).
[33] M. Duraisamy and A. Datta, J. High Energy Phys. 09 (2013) 059.
[34] M. Duraisamy, P. Sharma, and A. Datta, Phys. Rev. D **90**, 074013 (2014).
[35] D. Becirevic, S. Fajfer, I. Nisandzic, and A. Tayduganov, Nucl. Phys. **B946**, 114707 (2019).
[36] Z. Ligeti, M. Papucci, and D. J. Robinson, J. High Energy Phys. 01 (2017) 083.
[37] M. A. Ivanov, J. G. Körner, and C.-T. Tran, Phys. Rev. D **95**, 036021 (2017).
[38] F. U. Bernlochner, Z. Ligeti, M. Papucci, and D. J. Robinson, Phys. Rev. D **95**, 115008 (2017); **97**, 059902 (E) (2018).
[39] M. Blanke, A. Crivellin, S. de Boer, T. Kitahara, M. Moscati, U. Nierste, and I. Nišandžić, Phys. Rev. D **99**, 075006 (2019).
[40] S. Bhattacharya, S. Nandi, and S. Kumar Patra, Eur. Phys. J. C **79**, 268 (2019).
[41] P. Colangelo and F. De Fazio, J. High Energy Phys. 06 (2018) 082.
[42] C. Murgui, A. Peñuelas, M. Jung, and A. Pich, J. High Energy Phys. 09 (2019) 103.
[43] R.-X. Shi, L.-S. Geng, B. Grinstein, S. Jäger, and J. Martin Camalich, J. High Energy Phys. 12 (2019) 065.
[44] A. K. Alok, D. Kumar, S. Kumbhakar, and S. Uma Sankar, Nucl. Phys. **B953**, 114957 (2020).
[45] R. Mandal, C. Murgui, A. Peñuelas, and A. Pich, J. High Energy Phys. 08 (2020) 022.
[46] S. Kumbhakar, Nucl. Phys. **B963**, 115297 (2021).
[47] S. Iguro and R. Watanabe, J. High Energy Phys. 08 (2020) 006.
[48] B. Bhattacharya, A. Datta, S. Kamali, and D. London, J. High Energy Phys. 07 (2020) 194.
[49] N. Penalva, E. Hernández, and J. Nieves, J. High Energy Phys. 06 (2021) 118.
[50] N. Penalva, E. Hernández, and J. Nieves, Phys. Rev. D **102**, 096016 (2020).
[51] R. Dutta and A. Bhol, Phys. Rev. D **96**, 076001 (2017).
[52] J. Harrison, C. T. Davies, and A. Lytle (LATTICE-HPQCD Collaboration), Phys. Rev. Lett. **125**, 222003 (2020).
[53] R. Dutta, Phys. Rev. D **93**, 054003 (2016).
[54] S. Shivashankara, W. Wu, and A. Datta, Phys. Rev. D **91**, 115003 (2015).
[55] X.-Q. Li, Y.-D. Yang, and X. Zhang, J. High Energy Phys. 02 (2017) 068.
[56] A. Datta, S. Kamali, S. Meinel, and A. Rashed, J. High Energy Phys. 08 (2017) 131.
[57] A. Ray, S. Sahoo, and R. Mohanta, Phys. Rev. D **99**, 015015 (2019).
[58] F. U. Bernlochner, Z. Ligeti, D. J. Robinson, and W. L. Sutcliffe, Phys. Rev. D **99**, 055008 (2019).
[59] E. Di Salvo, F. Fontanelli, and Z. J. Ajaltouni, Int. J. Mod. Phys. A **33**, 1850169 (2018).
[60] M. Blanke, A. Crivellin, T. Kitahara, M. Moscati, U. Nierste, and I. Nišandžić, Phys. Rev. D **100**, 035035 (2019).

[61] P. Böer, A. Kokulu, J.-N. Toelstede, and D. van Dyk, J. High Energy Phys. 12 (2019) 082.
[62] X.-L. Mu, Y. Li, Z.-T. Zou, and B. Zhu, Phys. Rev. D **100**, 113004 (2019).
[63] Q.-Y. Hu, X.-Q. Li, Y.-D. Yang, and D.-H. Zheng, J. High Energy Phys. 02 (2021) 183.
[64] N. Penalva, E. Hernández, and J. Nieves, Phys. Rev. D **100**, 113007 (2019).
[65] N. Penalva, E. Hernández, and J. Nieves, Phys. Rev. D **101**, 113004 (2020).
[66] R. Aaij *et al.* (LHCb Collaboration), Phys. Rev. Lett. **128**, 191803 (2022).
[67] W. Detmold, C. Lehner, and S. Meinel, Phys. Rev. D **92**, 034503 (2015).
[68] Marco Pappagallo (private communication).
[69] N. Penalva, E. Hernández, and J. Nieves, J. High Energy Phys. 04 (2022) 026.
[70] F. U. Bernlochner, Z. Ligeti, M. Papucci, and D. J. Robinson, arXiv:2206.11282.
[71] N. Penalva, E. Hernández, and J. Nieves, J. High Energy Phys. 10 (2021) 122.
[72] P. Asadi, A. Hallin, J. Martin Camalich, D. Shih, and S. Westhoff, Phys. Rev. D **102**, 095028 (2020).
[73] S. Meinel and G. Rendon, Phys. Rev. D **103**, 094516 (2021).
[74] S. Meinel and G. Rendon, Phys. Rev. D **105**, 054511 (2022).
[75] A. K. Leibovich and I. W. Stewart, Phys. Rev. D **57**, 5620 (1998).
[76] M.-L. Du, E. Hernández, and J. Nieves, arXiv:2207.02109.
[77] J. Nieves and R. Pavao, Phys. Rev. D **101**, 014018 (2020).
[78] J. Nieves, R. Pavao, and S. Sakai, Eur. Phys. J. C **79**, 417 (2019).
[79] C. Itzykson and J. B. Zuber, *Quantum Field Theory*, International Series In Pure and Applied Physics (McGraw-Hill, New York, 1980).
[80] K. Kiers and A. Soni, Phys. Rev. D **56**, 5786 (1997).
[81] R. Alonso, A. Kobach, and J. Martin Camalich, Phys. Rev. D **94**, 094021 (2016).
[82] R. Alonso, J. Martin Camalich, and S. Westhoff, Phys. Rev. D **95**, 093006 (2017).
[83] M. Tanaka and R. Watanabe, Phys. Rev. D **82**, 034027 (2010).
[84] M. Papucci and D. J. Robinson, Phys. Rev. D **105**, 016027 (2022).
[85] R. Mertig, M. Böhm, and A. Denner, Comput. Phys. Commun. **64**, 345 (1991).
[86] V. Shtabovenko, R. Mertig, and F. Orellana, Comput. Phys. Commun. **207**, 432 (2016).
[87] V. Shtabovenko, R. Mertig, and F. Orellana, Comput. Phys. Commun. **256**, 107478 (2020).
[88] Wolfram Research, Inc., Mathematica, Version 12.3, Champaign, IL, 2021.